Ions and Solvent (Water) at Electrochemical Interfaces

- Introduction
- Historical Perspective
- Models of the EDL
- Experimental Methods used to probe the EDL
  - thermodynamics on Hg and Au
  - capacitance / impedance
  - in-situ spectroscopic methods
- even more complex interfaces

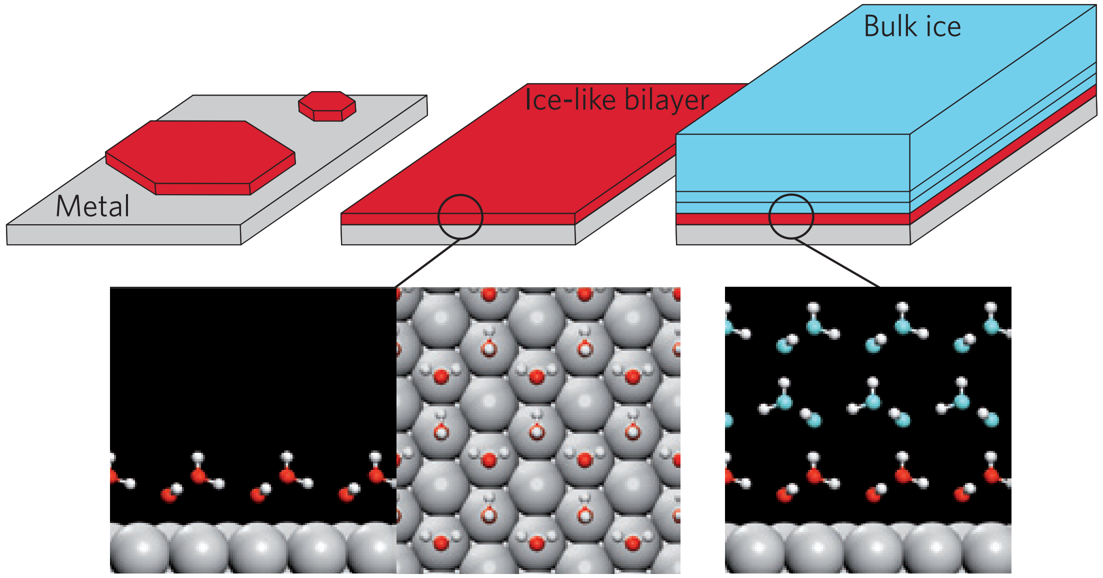

Carrasco, J.; Hodgson, A.; Michaelides, A. A Molecular Perspective of Water at Metal Interfaces. Nature materials 2012, 11 (8), 667–674.

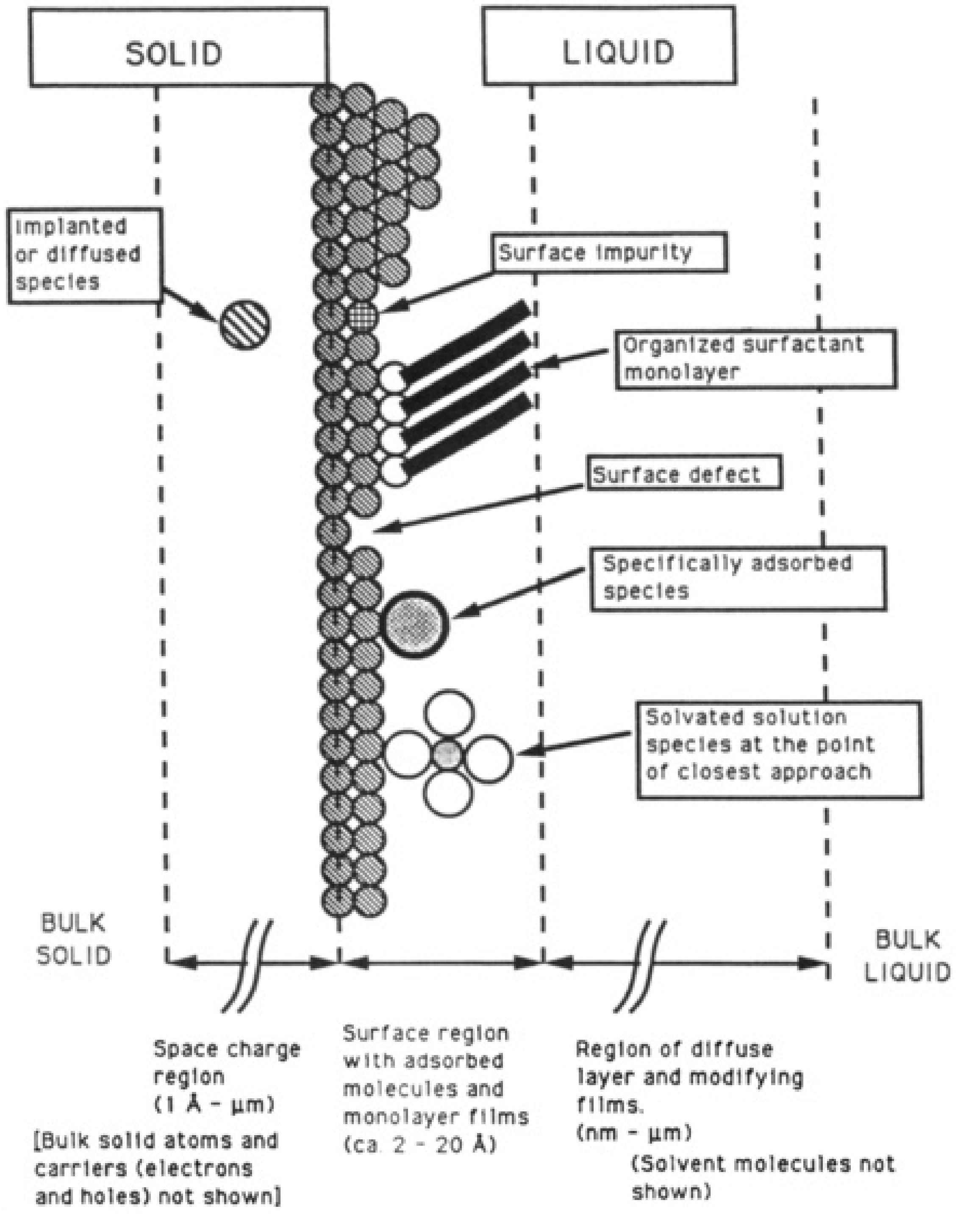

Figure 1. Schematic representation of the liquid–solid interfacial region showing possible species and features.[346]

Bard, A. J.; Abruna, H. D.; Chidsey, C. E. The Electrode/Electrolyte Interface-a Status Report. The Journal of Physical Chemistry 1993, 97 (28), 7147–7173.

Current Electrochemical Systems of Interest

- Electrochemical Super-Capacitors
  - modelling the EDL in porous materials
- Power Devices: Fuel Cells and Batteries
  - modelling the ionic distribution and impact on reduction/oxidation rates, potential distribution near nanoporous electrodes
- Oxide / semi-conducting electrodes
  - photoelectrochemical devices, combination: EDL and space charge layer, nanostructured electrodes
- Modified electrode surfaces: Sensors
  - adsorption of alkylthiol with charged functional groups (COOH, NH_2)
  - DNA / polyelectrolyte modified surfaces
  - adsorbed lipids: modelling biomembrane, creating sensors

The Electrode /Electrolyte Interface

- initial model was combination of Helmholtz, Gouy, Chapman and Stern which treated the electrode interface as plates or as capacitors in series
- the thickness of these layers were defined by the solvent and adsorbed ions (with or without hydration shell)
- developed and useful at low ionic strength

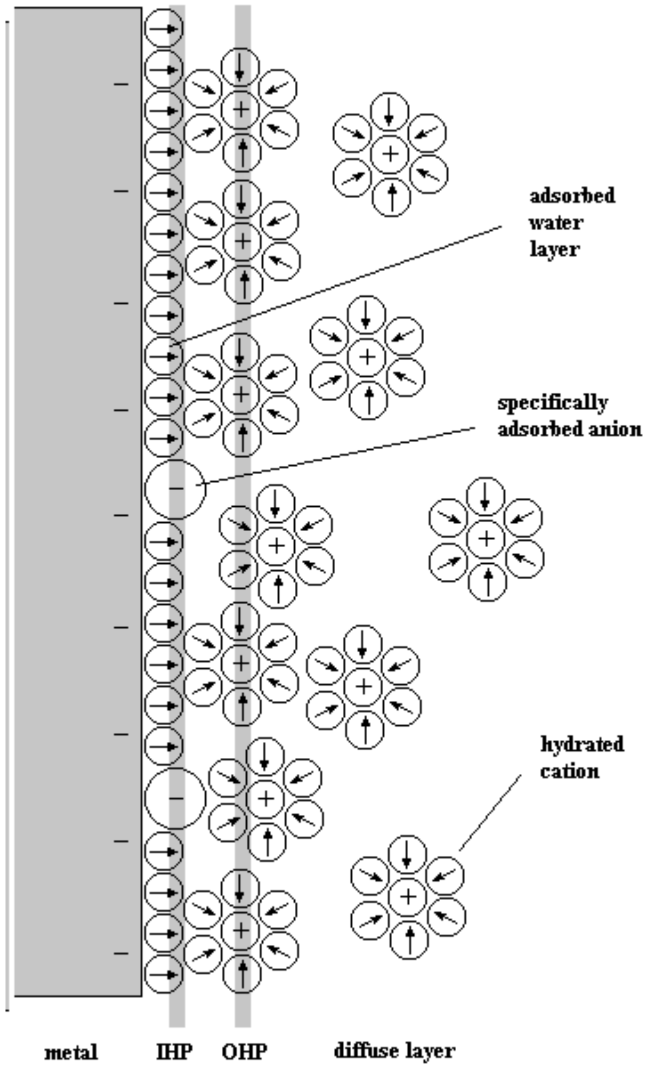

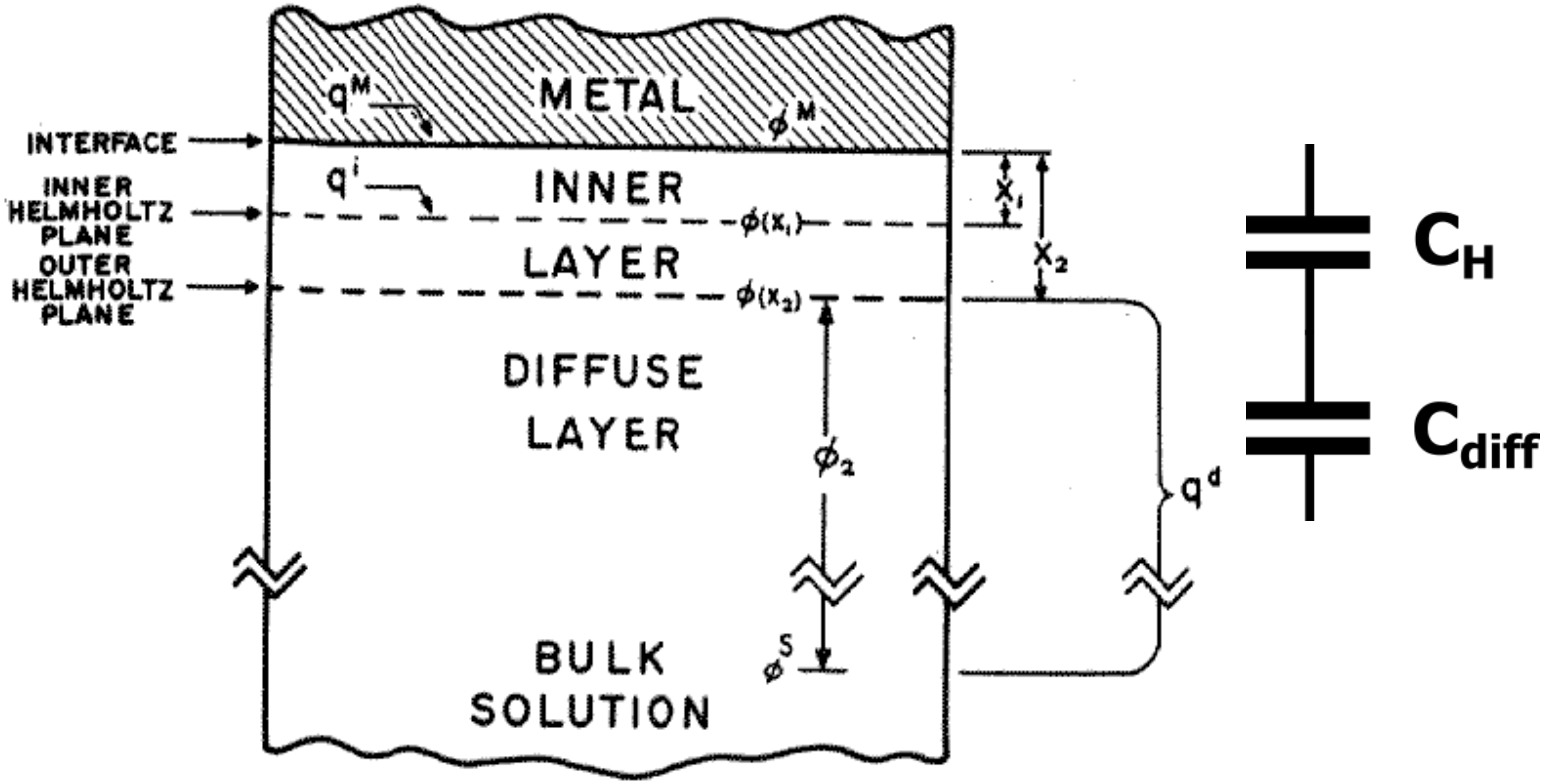

GCS approach for non-adsorbing electrolytes

- excess charge on the metal exists in a thin layer at the metal surface
- for non-adsorbing electrolytes:
  - only solvent in the Helmholtz layer
  - the compensating ionic charge exists in the diffuse layer
  - diffuse layer is much thicker than charge on the metal
  - water is considered as continuum with constant dielectric constant

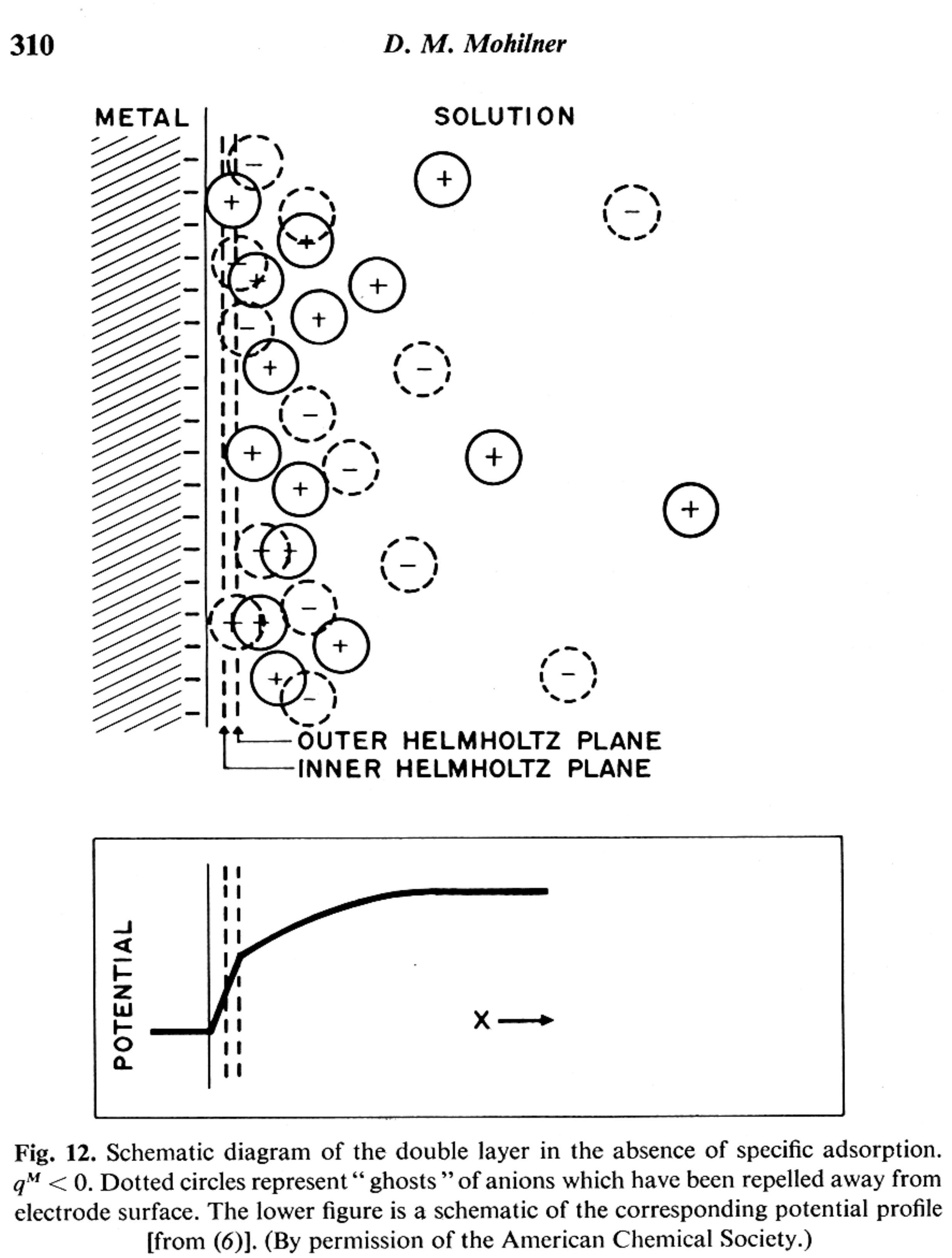

310 *D. M. Mohilner*

Fig. 12. Schematic diagram of the double layer in the absence of specific adsorption. $q^M < 0$. Dotted circles represent "ghosts" of anions which have been repelled away from electrode surface. The lower figure is a schematic of the corresponding potential profile [from (6)]. (By permission of the American Chemical Society.)

GCS theory for EDL

- the GCS model solves the PB equation resulting in an expression for the potential drop away from the electrode surface
  - dielectric is constant
  - ions are point charges
  - no specific adsorption (eg no chemical interaction between anions, cations and the metal surface, no ions in the inner layer, just solvent)

$$\phi_M = -\left(\frac{d\phi}{dx}\right)_{x=x_2} x_2 + \phi_2 \qquad \left(\frac{d\phi}{dx}\right)_{x=x_2} = -\left(\frac{8RTc_{\text{bulk}}}{\varepsilon\varepsilon_o}\right)^{1/2} \sinh\left(\frac{zF\phi_2}{2RT}\right)$$

Potential decay from metal surface (ϕ_2 = 0.25V)

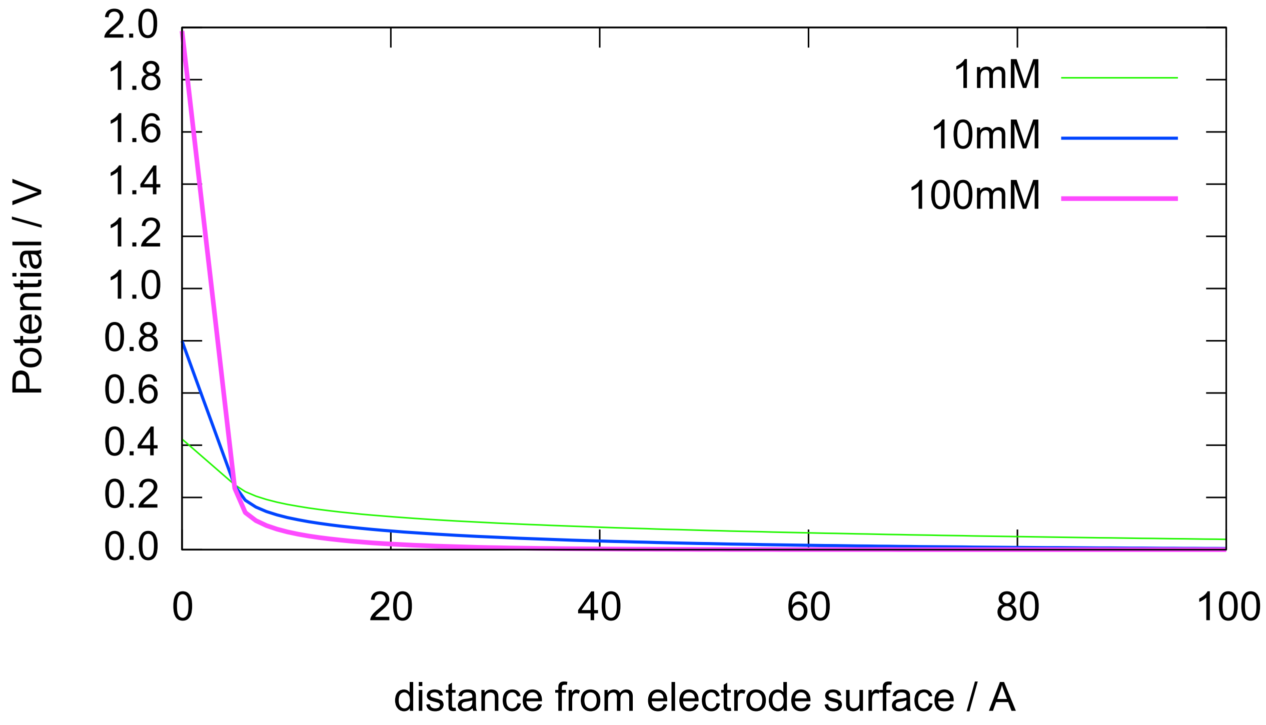

ϕ_2 for z=1 z:z electrolyte

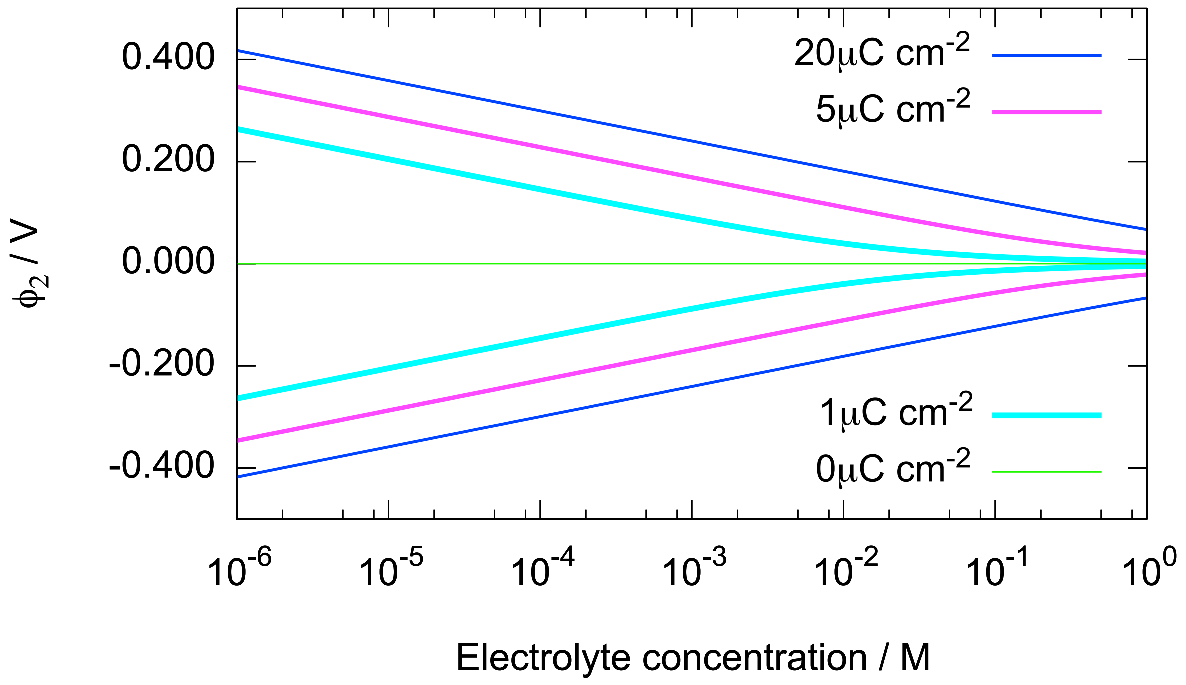

Real Electrode /Electrolyte Interfaces: Hg | water

- thermodynamic study of the structure of an electrified interface was pioneered by Grahame, Miller and Frumkin following Lippmann, Gibbs, Gouy, Chapman
- these careful thermodynamic measurements were performed on Hg electrodes
  - surface tension vs E
  - ideal system - smooth surface, easily cleaned/regenerated
  - changes in the surface tension of the Hg / electrolyte surface
  - revealed parabolic curves in keeping with capacitance model of the interface
  - max is at potential of zero charge(pzc)
  - non-adsorbing electrolyte gives a symmetric parabola

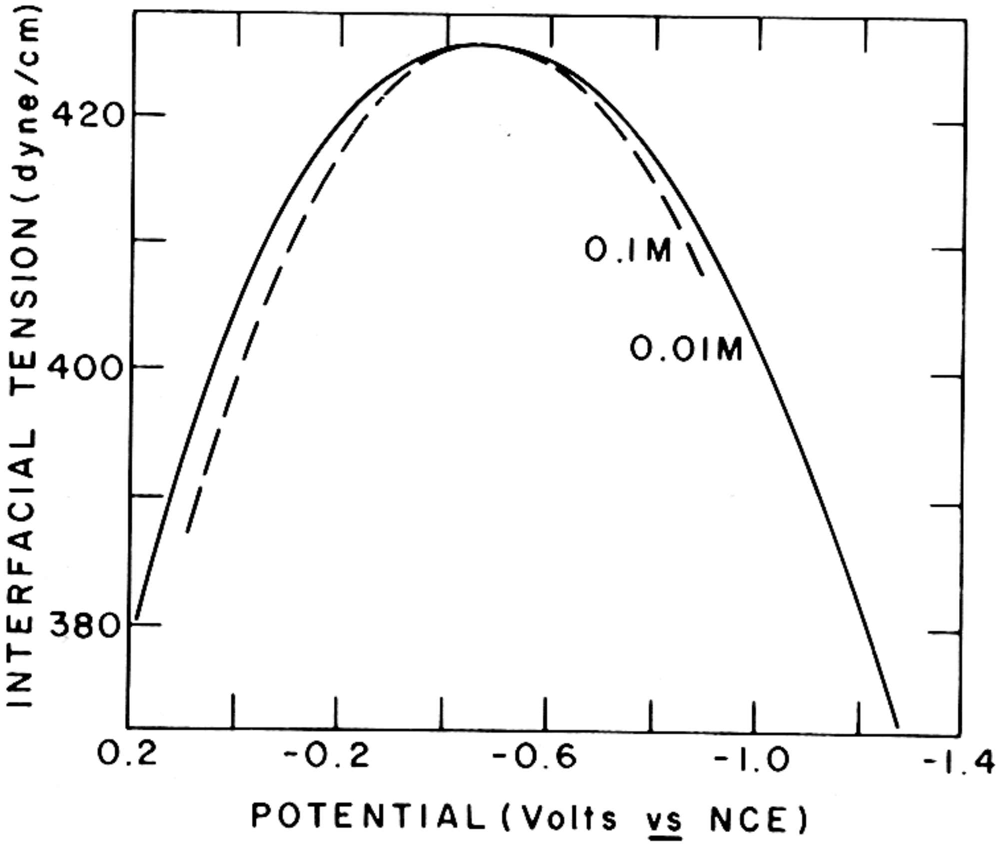

FIG. II 10a ELECTROCAPILLARY CURVES FOR NaF SOLUTIONS (D.C. Grahame and B.A. Soderberg, Tech. Report No. 14, ONR (1954); J. Lawrence, R. Parsons and R. Payne, J. Electroanal. Chem. 16, 193 (1968)).

$$-\partial\gamma = \sigma_M \partial E$$

$$\gamma = \gamma_{\max} - \frac{\varepsilon\varepsilon_o}{2x_2}(E - E_{pzc})^2 = \gamma_{\max} - \frac{C}{2}(E - E_{pzc})^2$$

Non-specific adsorbing electrolyte: Hg | NaF

- thermodynamics can be used to determine if system is ideal, without specific adsorption of the anion: Hg | NaF
- p.z.c. does not shift with [NaF]: Esin-Markov coefficient is constant at negative potentials

$$-\left(\frac{\partial E_+}{\partial \mu_{MX}}\right)_{\sigma_M} = \left(\frac{\partial \Gamma_-}{\partial \sigma_M}\right)_{\mu_{MX}}$$

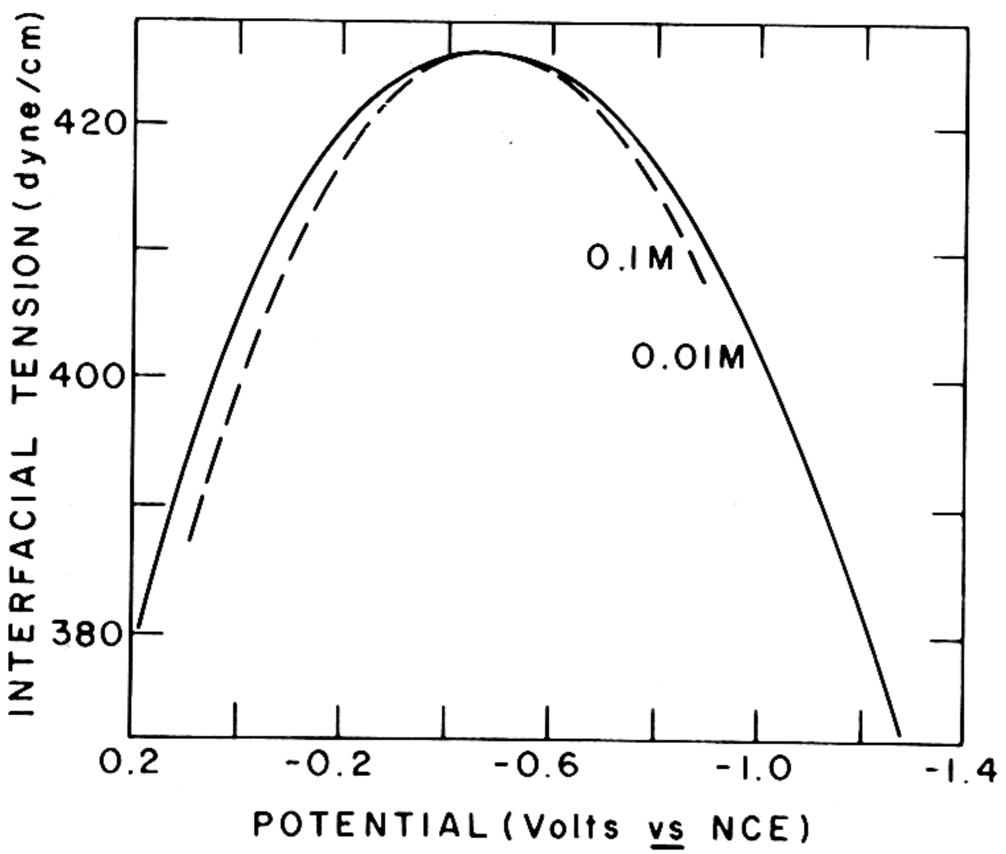

FIG. II 10a ELECTROCAPILLARY CURVES FOR NaF SOLUTIONS (D.C. Grahame and B.A. Soderberg, Tech. Report No. 14, ONR (1954); J. Lawrence, R. Parsons and R. Payne, J. Electroanal. Chem. 16, 193 (1968)).

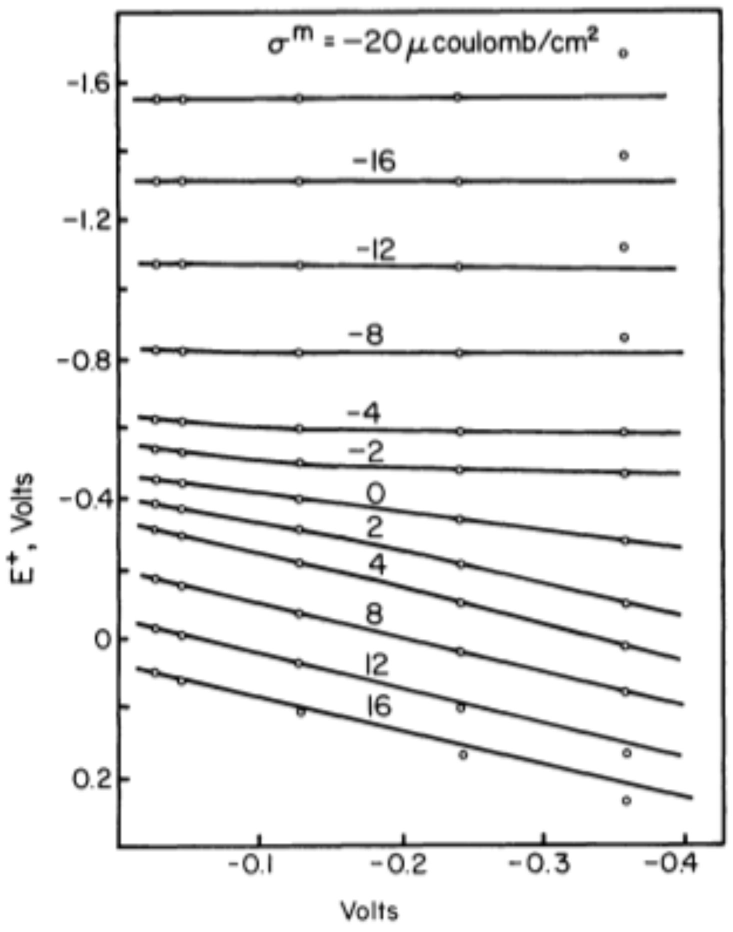

Figure 10. Essin and Markov plots for NaF solutions calculated from the data of Grahame.[69]

Hg | NaF: Electrochemical Capacitance

- interfacial capacitance is easily measured
- related to surface tension
- minimum at p.z.c. for low [electrolyte], due to minimum in C_d
- C_i (or C_H) is almost constant, changes due to solvent

$$\sigma_M = \left(\frac{d\gamma}{dE}\right)_\mu \qquad C = \left(\frac{d^2\gamma}{d^2E}\right)_\mu$$

$$\frac{1}{C_{dl}} = \frac{1}{C_i} + \frac{1}{C_d} \qquad \frac{1}{C_{dl}} = \frac{x_2}{\epsilon\epsilon_o} + \frac{1}{(2\varepsilon\varepsilon_o z^2 F^2 c_{\text{bulk}}/RT)^{1/2}\cosh(zF\phi_2/2RT)}$$

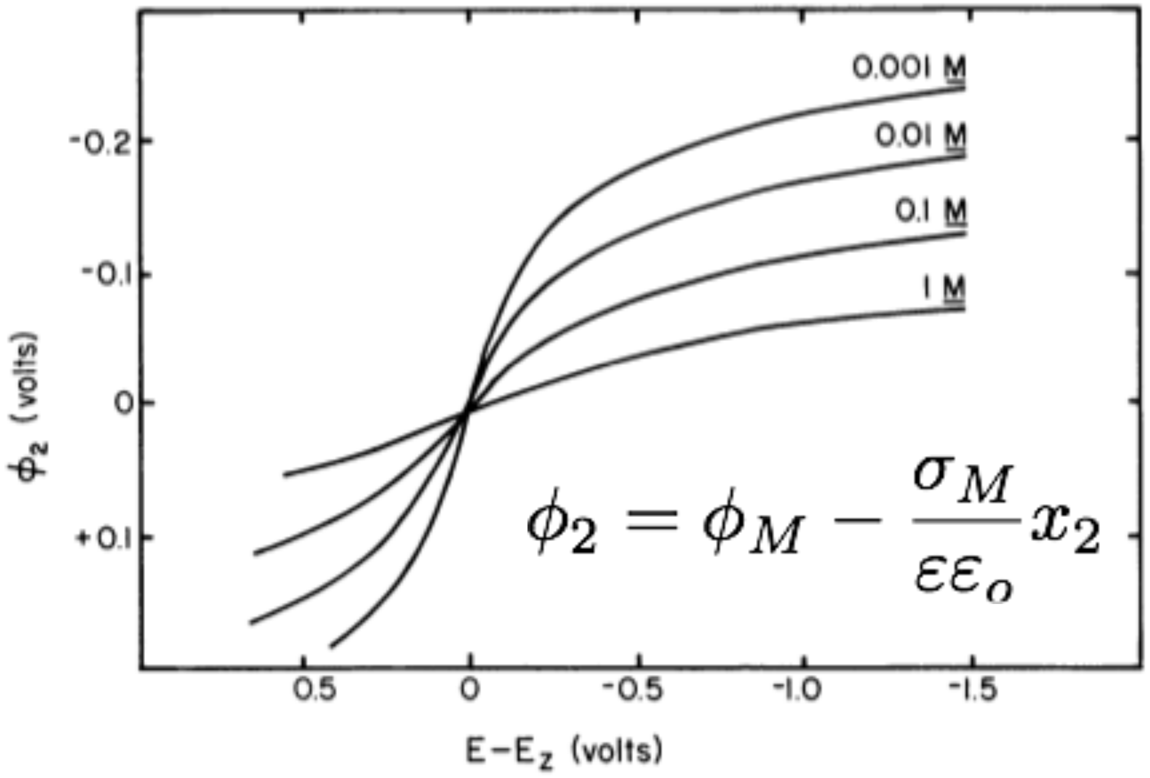

$$\phi_2 = \phi_M - \frac{\sigma_M}{\varepsilon\varepsilon_o}x_2$$

Figure 16. Variations of the potential ϕ_2 between the plane of closest approach and the bulk of the solution with $E - E_z$ for the mercury in sodium fluoride solutions at 25°C. Calculated from Grahame's data.[62,68,20]

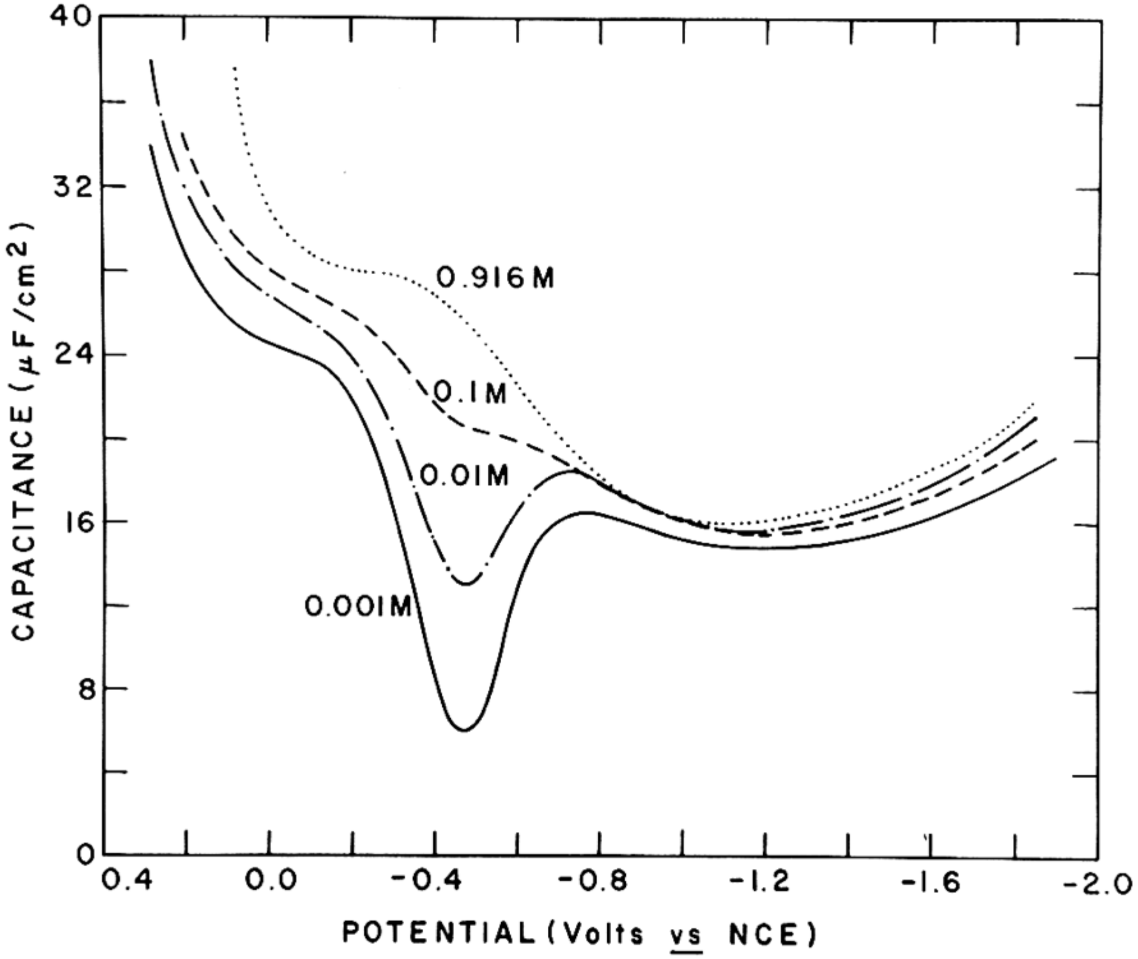

Helmholtz / Inner layer Capacitance

- the metal | inner layer capacitance C_i (or C_H):
- metal is modelled as jellium with electron spillover into the solution (best for metals described with non-localized sp bands)
- contributes to changes in C_H with charge and nature of the metal

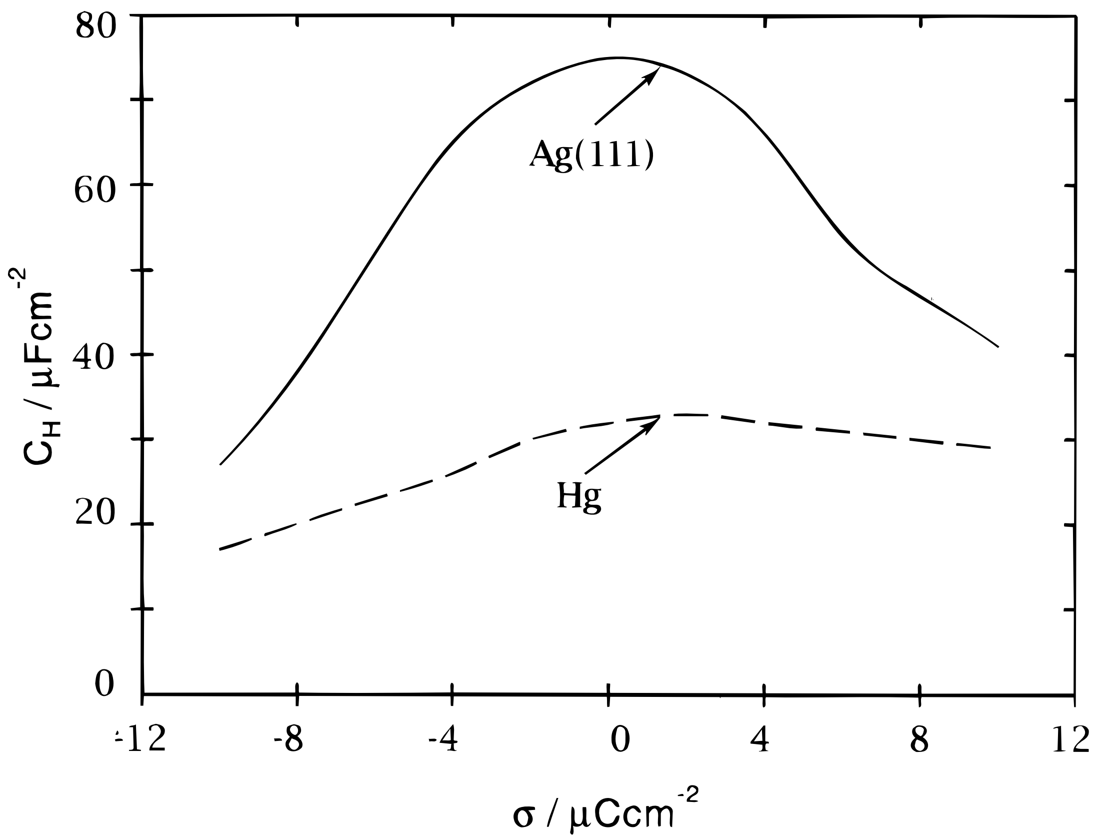

Figure 3. Helmholtz capacity as a function of the electrode charge for mercury and Ag(111) in contact with an aqueous solution of ions that are not specifically adsorbed.

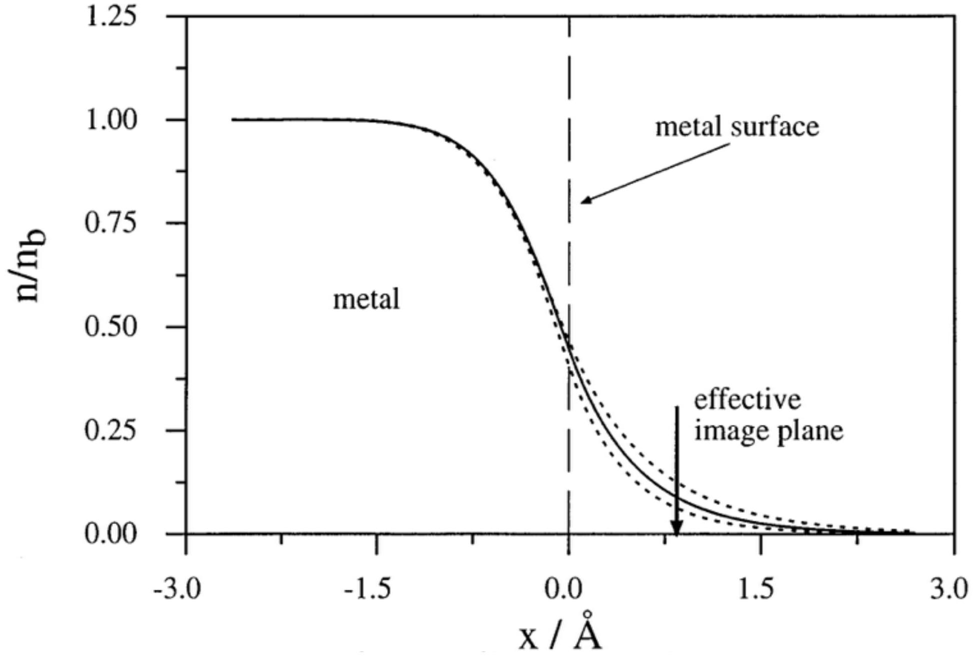

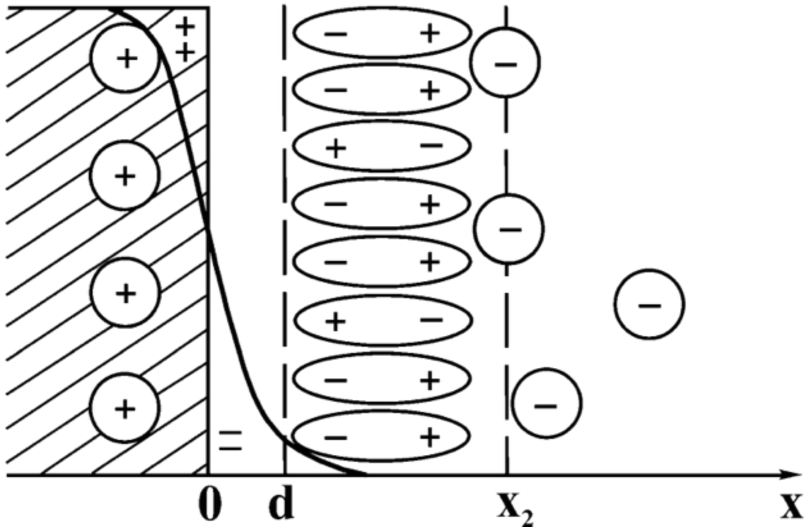

Schmickler, W. Electronic Effects in the Electric Double Layer. Chem. Rev. 1996, 96 (8), 3177–3200.

Damaskin, B. B.; Petrii, O. A. Historical Development of Theories of the Electrochemical Double Layer. Journal of Solid State Electrochemistry 2011, 15 (7-8), 1317–1334.

Work Function, Surface Dipole and PZC

- the role of the metal and its surface dipole (χ_M) due to electron spillover: the metal electrode's work function $-\Phi = \mu_e + z_e e_o \chi_M$ is correlated to p.z.c.
- in terms of C_H:

$$\frac{1}{C_H} = \frac{1}{C_{metal}} + \frac{1}{C_{sol}} \qquad \frac{1}{C_{metal}} = \frac{\partial \chi_M}{\partial \sigma_M}$$

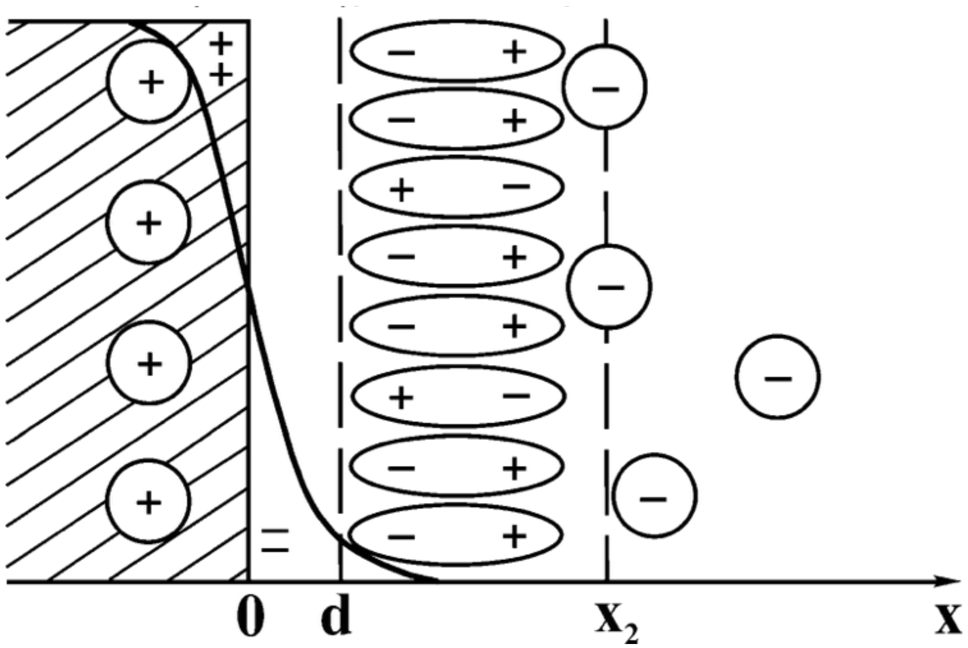

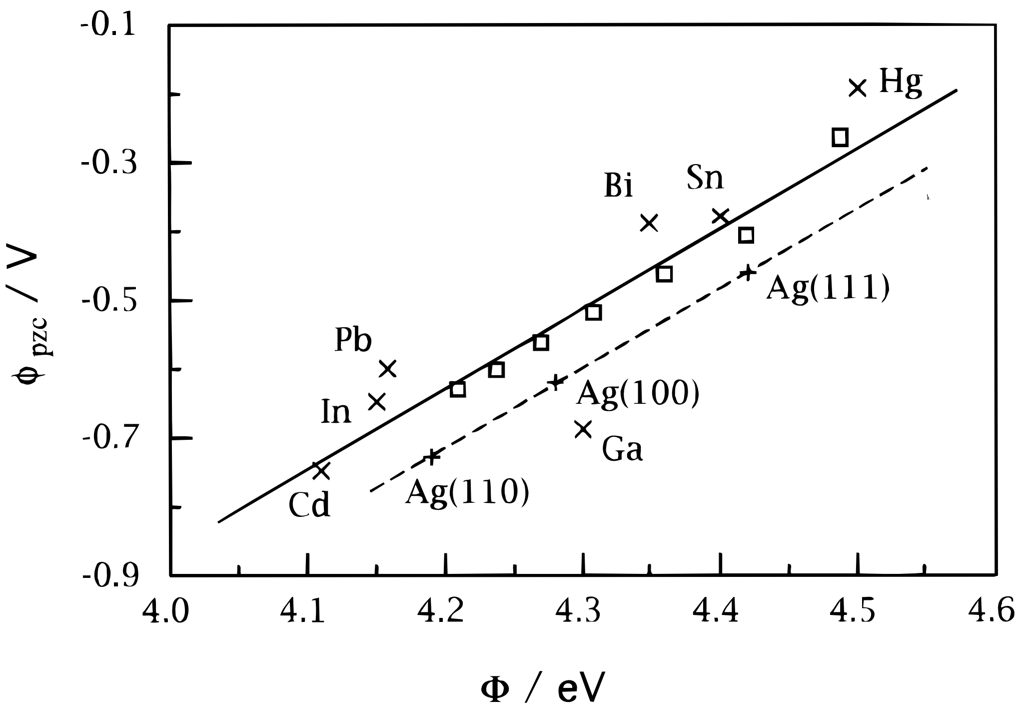

Figure 2. Potential of zero charge of several groups of metals versus their work function. The sp metals are indicated by ×, the work functions of the solid metals are for polycrystalline samples; data were taken from Trasatti.[7] The indium amalgams are indicated by □; these data are from ref 11. The solid line indicates the correlation for the sp metal including the amalgams; the dashed line is for the silver surfaces.

Schmickler, W. Electronic Effects in the Electric Double Layer. Chem. Rev. 1996, 96 (8), 3177–3200.

Damaskin, B. B.; Petrii, O. A. Historical Development of Theories of the Electrochemical Double Layer. Journal of Solid State Electrochemistry 2011, 15 (7-8), 1317–1334.

Metal & first layer of solvent

- solvent and ions also play a role in the value of C_H
- position of charge plane at the inner layer (x_2) can change with charge on the metal
- orientation of water at the surface is generally thought to be a simple layer of dipoles, changing directions as the charge changes sign

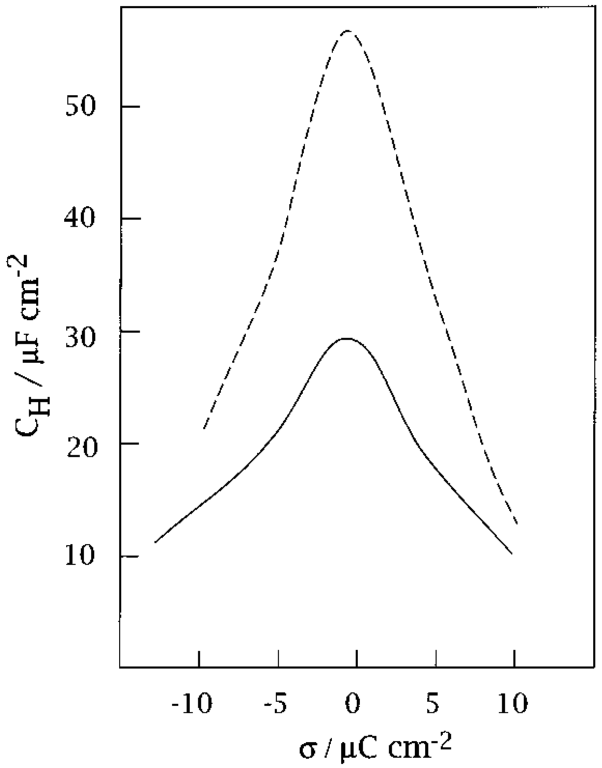

Figure 35. The Helmholtz capacity as function of the charge density. The dashed curve is for a bulk electronic density of $n_b = 0.02$ au, the full curve for $n_b = 0.01$ au; based on the work Schmickler and Henderson.[97]

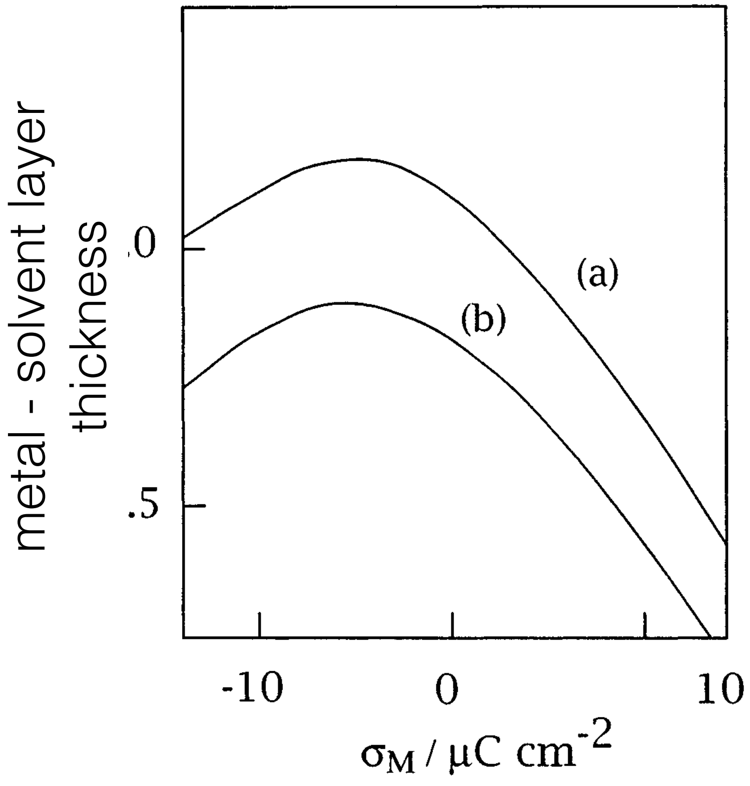

Fig. 11. Metal–solvent separation s as a function of the surface-charge density for two different choices of pseudopotentials [54].

Schmickler, W. Electronic Effects in the Electric Double Layer. Chem. Rev. 1996, 96 (8), 3177–3200.

Damaskin, B. B.; Petrii, O. A. Historical Development of Theories of the Electrochemical Double Layer. Journal of Solid State Electrochemistry 2011, 15 (7-8), 1317–1334.

More complex: Adsorbing electrolyte

- for other electrolytes parabola are asymmetric and the p.z.c. depends on anion
- specific adsorption of anion - chemical interaction with metal
- modifies potential at the interface and into solution
- models of interface more complex
  - electrosorption valency
  - super-equivalent adsorption

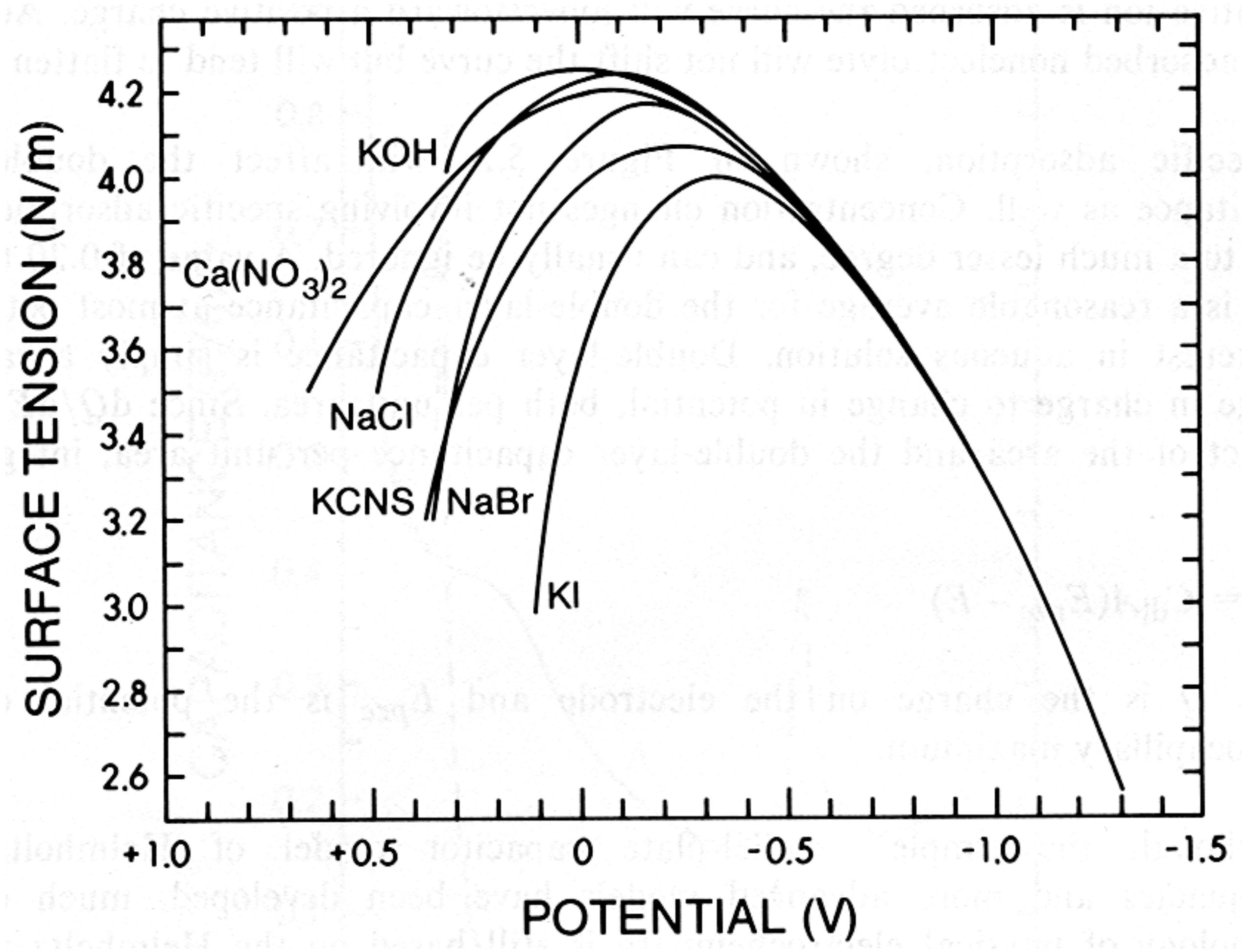

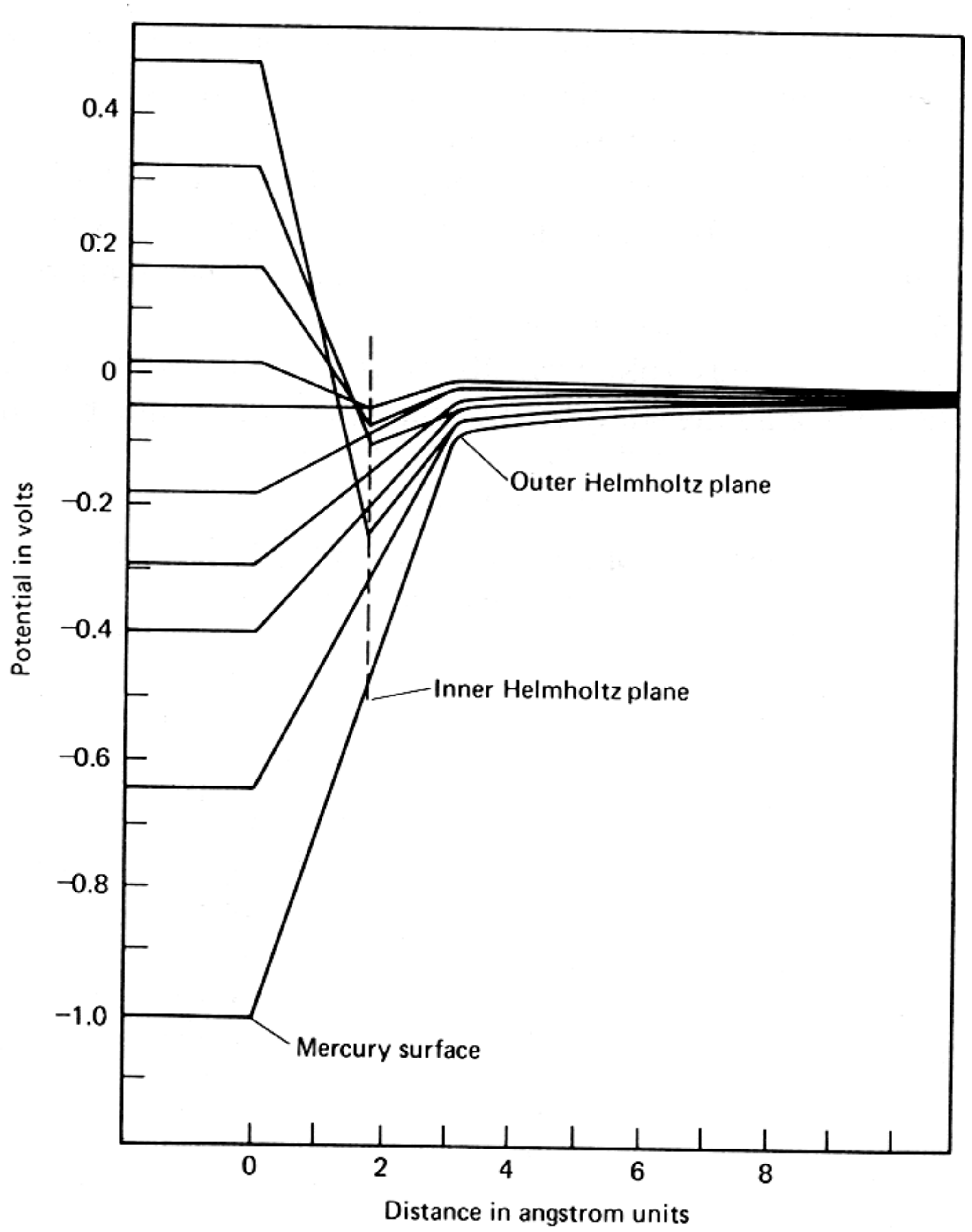

Specific Adsorption of Anions

- specific adsorption of halide anions (Cl^-, I^-, Br^-) on Hg
- shows a super equivalent amount of Br^- on the +ve charged surface
- shift in p.z.c. with [Br^-]: characteristic of specific adsorption
- due to extra chemical interaction between Hg and Br^-
- ions lose some of their solvation shell, centered in IHP ($x_1 < x_2$)

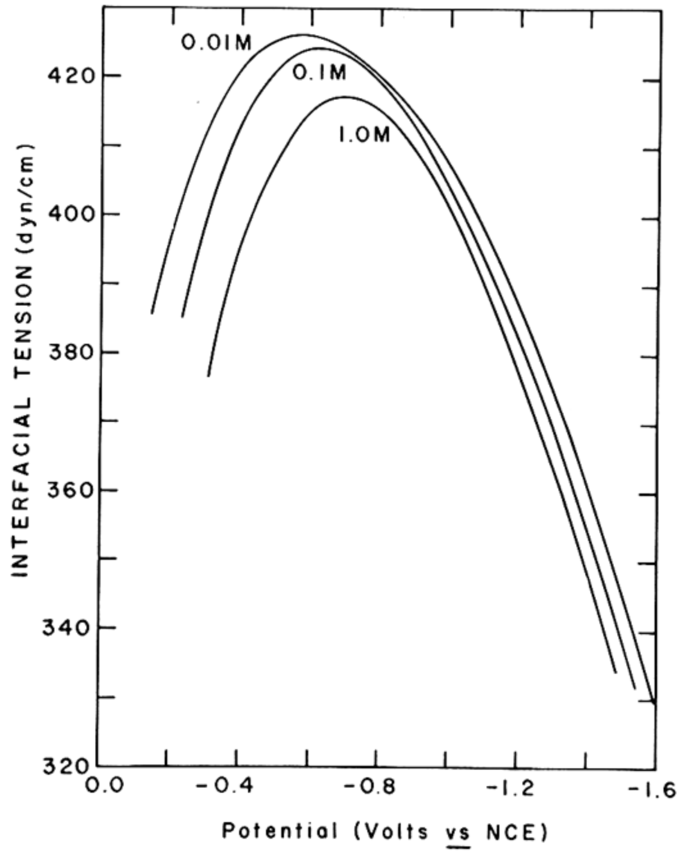

FIG. II 11a ELECTROCAPILLARY CURVES FOR KBr SOLUTIONS (J. Lawrence, R. Parsons and R. Payne, J. Electroanal. Chem. 16, 193 (1968)).

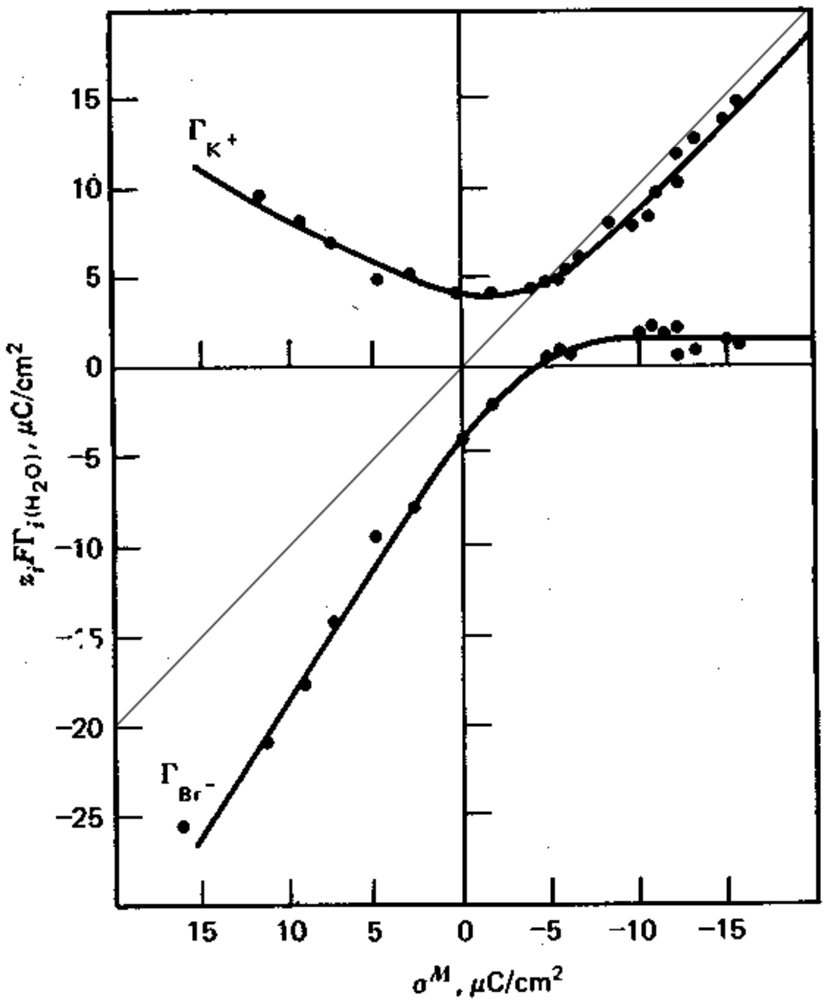

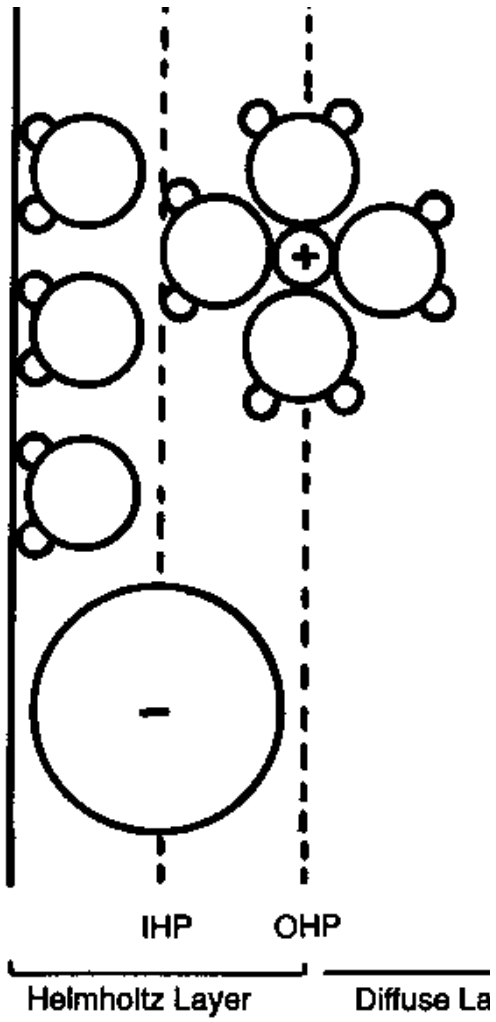

Electrosorption Valency

- a measure of the bonding between the ion and the surface is given by ‘electrosorption valency’

$$l_b = -z\left(\frac{\partial \sigma_M}{\partial \sigma_i}\right)_E = -z\left(\frac{\partial \sigma_M}{\partial \Gamma^i_{S,ads}}\right)_E$$

- measure of the avg number of electrons that are transferred to the electrode per adsorbed ion or molecule
- for ion adsorption, need an estimate of charge in diffuse layer: use GCS theory
- extra-thermodynamic & modelistic
- measure of the extent of electron transfer, or electron sharing due to adsorption
- solvent is displaced from the surface and reorientation must also be considered

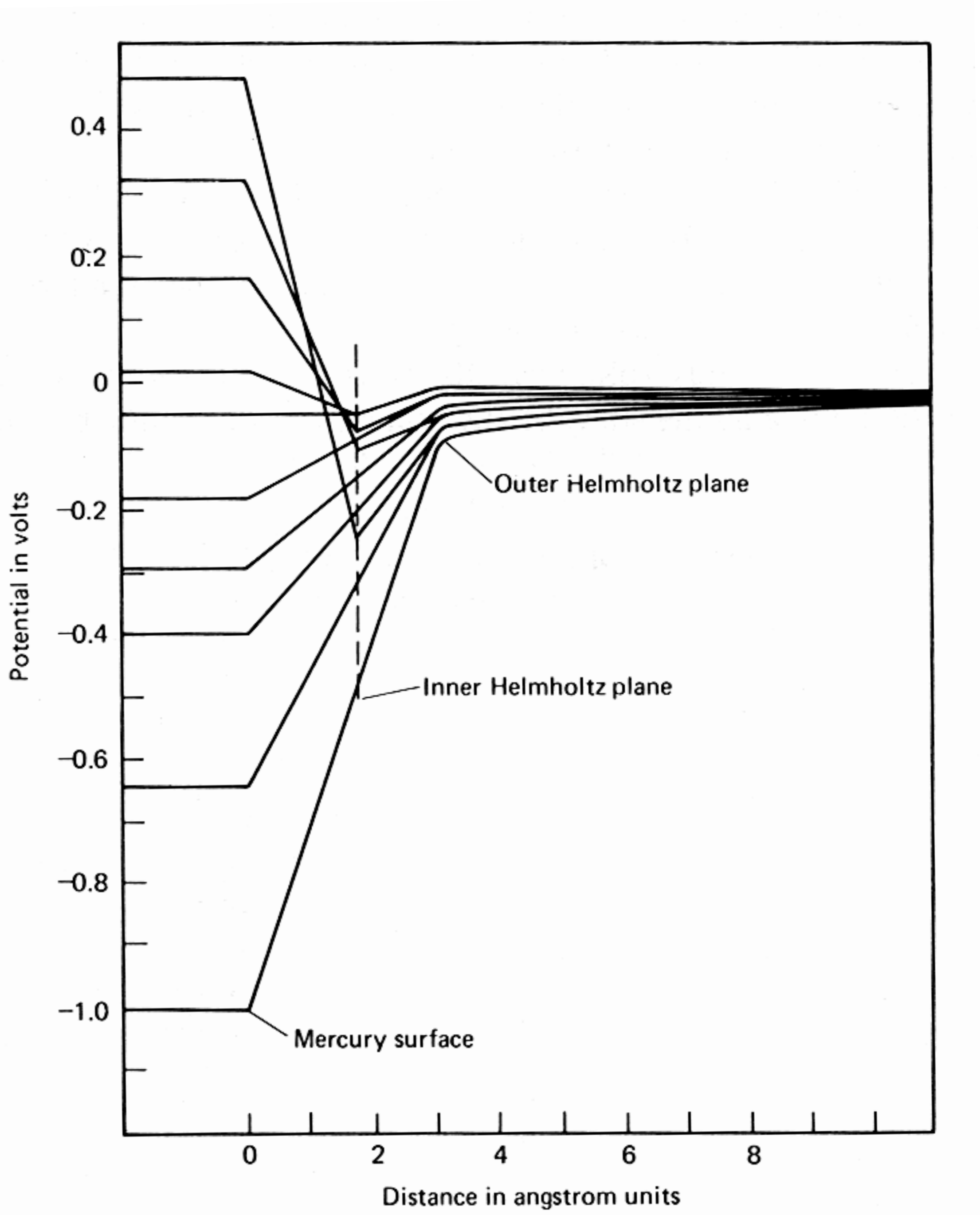

Figure 12.3.8
ofiles in the double layer for mercury in contact with 0.3 *M* NaCl i
tials given with respect to the PZC in NaF. [Reprinted with permi
me, *Chem. Rev.*, **41**, 441 (1947). Copyright 1947, Williams and Wi

Electrosorption Valency & Solvent

- potential decay away from the electrode surface is significantly changed
- solvent dipoles are also affected, respond to local changes in the E
- electrosorption valency influenced by the efficiency of solvent screening

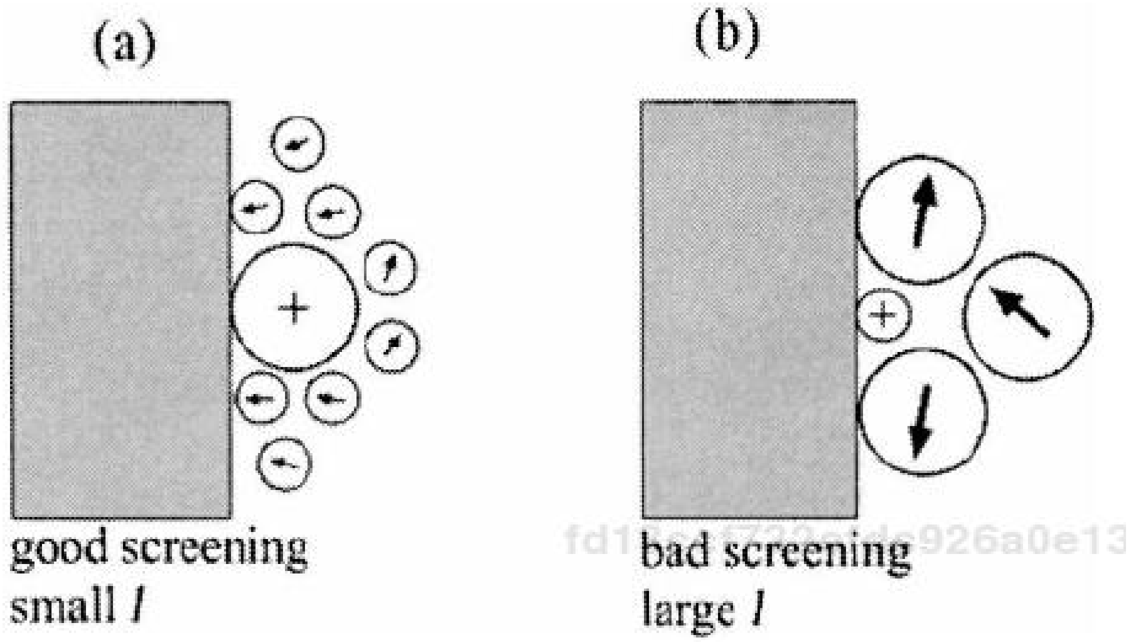

Figure 2. Schematic picture of the screening of an adsorbed cation by solvent molecules of different sizes with respect to that of the cation.

Guidelli, R.; Schmickler, W. Electrosorption Valency and Partial Charge Transfer. Modern Aspects of Electrochemistry 2005, 38 (Chapter 3), 303–371.

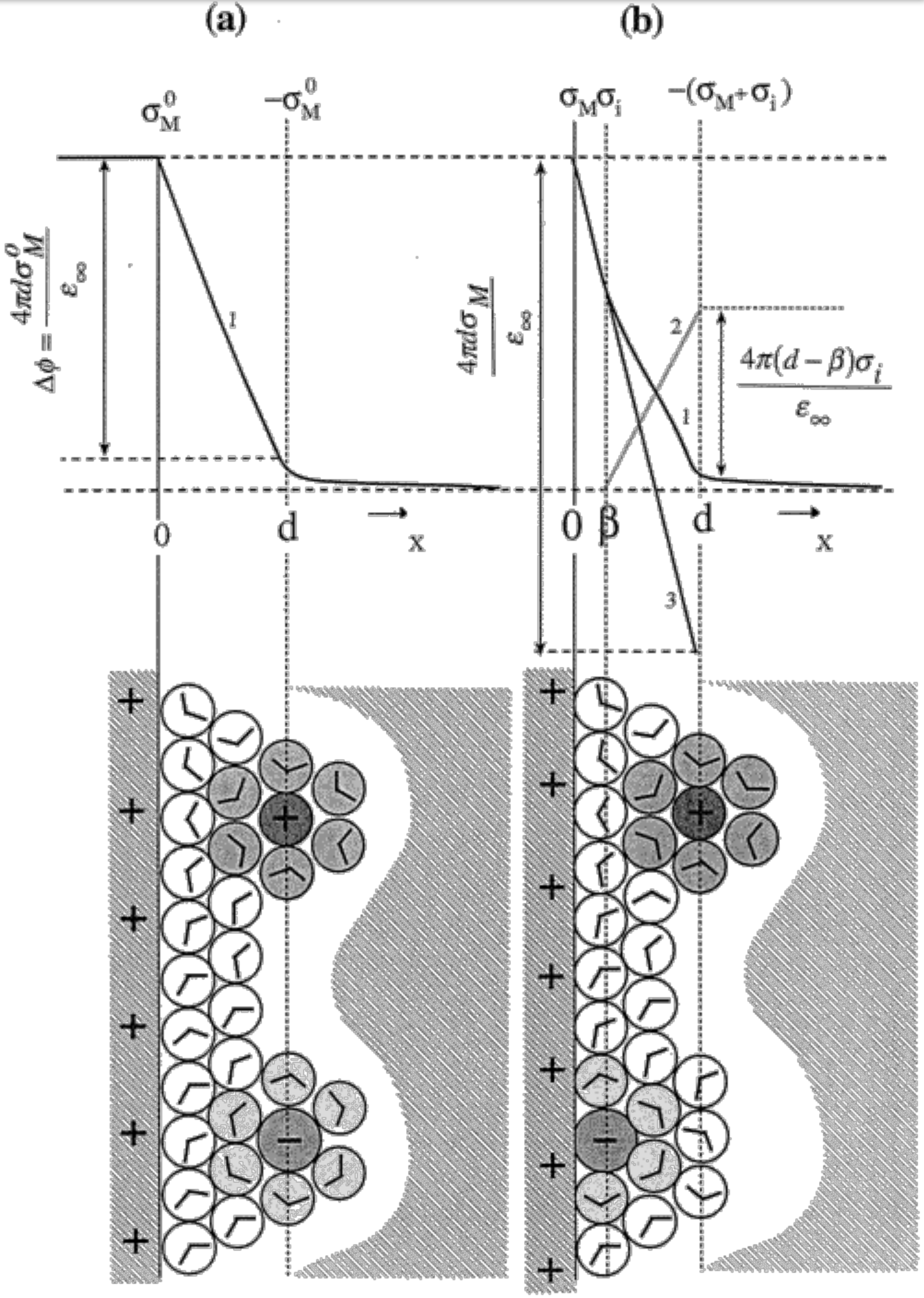

Electrosorption Valency and Partial Charge Transfer in Halide and Sulfide Adsorption on Ag(111) Maria Luisa Foresti, Massimo Innocenti, Francesca Forni, and, and Rolando Guidelli* *Langmuir* 1998 *14* (24), 7008-7016

Specific Adsorption on Solid Electrodes

- Hg is ideal, but solid metal surfaces are most often used
- adsorption of ions, orientation of solvent can have a dramatic impact on the electrocatalytic reactivity
  - eg. ORR on Pt(hkl) (110 > 111 > 100)
  - reactivity of nanoparticle surfaces differ in fuel cell
- modification of the potential drop from metal - solution impacts the driving force for electron transfer
- initial stages of metal deposition (eg Cu on Au)

specific adsorption impacts surface reconstruction (eg. Au(100))

Schmickler, W. Electronic Effects in the Electric Double Layer. Chem. Rev. 1996, 96 (8), 3177–3200.

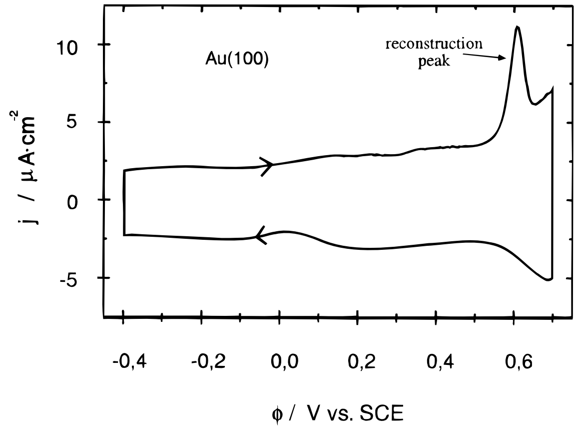

Figure 21. Current/potential curve (cyclic voltammogram) of a Au(100) surface in 10 mM $HClO_4$. The electrode has been prepared by flame annealing and was then immersed into the solution at a potential of −0.4 V vs SCE. Subsequently, the potential was scanned with a rate of 50 mV s^{-1} in the positive direction. At a potential of 0.7 V the direction of the sweep was reversed until the initial potential was reached again. The direction of the scan is indicated by an arrow.

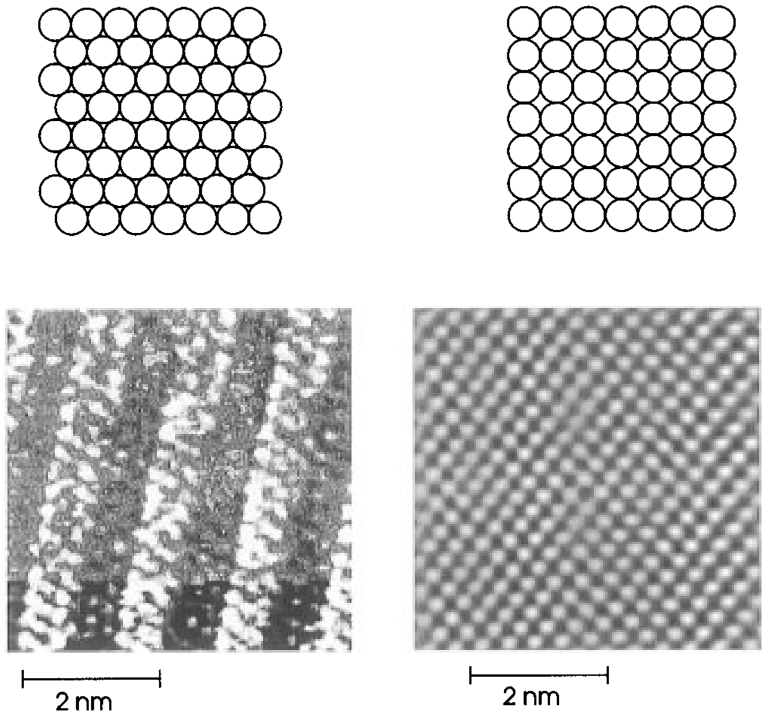

Figure 20. Surface structure of the reconstructed (left) and of the ideal (right) Au(100) surface. The upper drawings show the surface structures of the STM images below. On account of the misfit of the top layer with the bulk the reconstructed surface shows a surface corrugation. Courtesy of D. M. Kolb, Ulm.

Specific Adsorption on Au(111)

- adsorption studied on single crystals
- can use similar thermodynamic approach as with Hg
- use charge density instead of surface tension
- eg: Cl^- adsorption on Au(111)

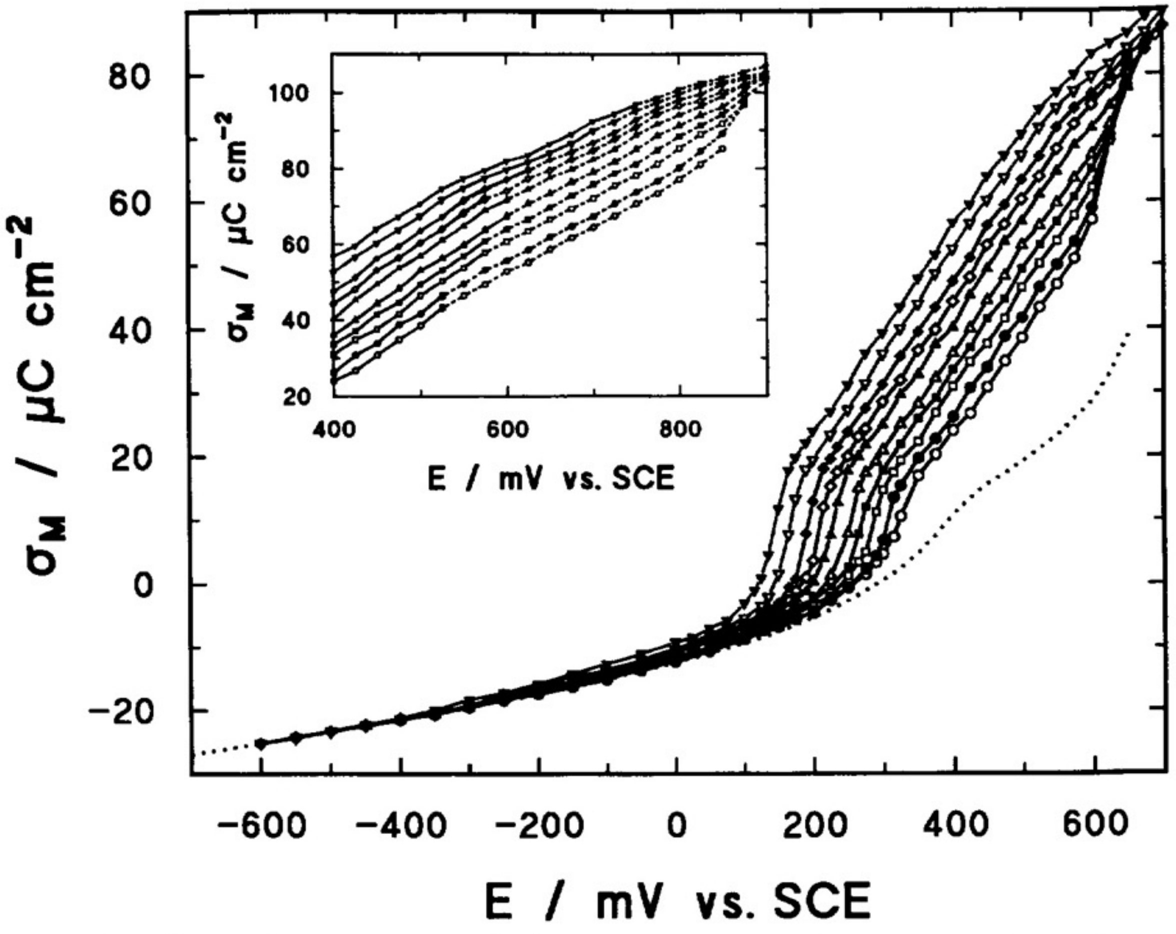

Fig. 2. Charge density versus electrode potential curves for the Au(111) electrode in pure 0.1 M $KClO_4$ solution (······) and with the following KC concentrations/mol dm^{-3}: ○ 5×10^{-6}; ● 10^{-5}; □ 2.5×10^{-5}; ■ 5×10^{-5}; △ 10^{-4}; ▲ 2.5×10^{-4}; ◇ 5×10^{-4}; ◆ 10^{-3}; ▽ 2.5×10^{-3}; ▼ 5×10^{-3}. The inset to Fig. 2 shows sections of the charge density curves measured for the positive potentials in the acidified electrolyte (0.1 M $KClO_4$ + 10^{-3} M $HClO_4$ + x M KCl).

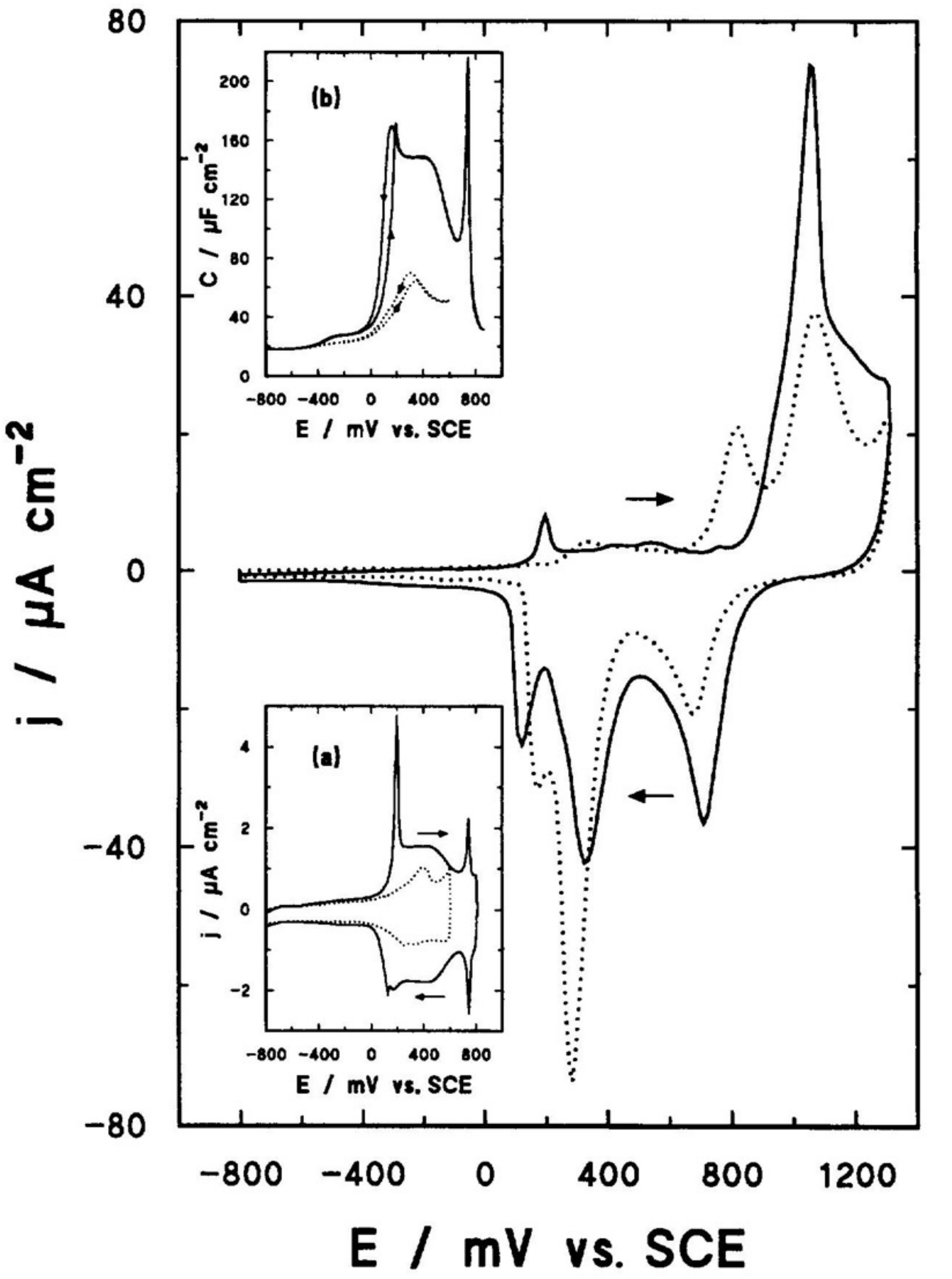

an Au(111) electrode in 0.1 M $KClO_4$ (······) and in 0.1 M $KClO_4$ + 10^{-3} M KCl (——
ble-layer sections of the CV curves recorded at a sweep rate of 10 mV s^{-1}. Inset (b) shows the
sing an ac perturbation of frequency 25 Hz and amplitude 5 mV rms at a sweep rate of 10 mV s

Specific Adsorption on Solid Electrodes

- Cl^- adsorption on Au(111): coverage, adsorption free energy determined via charge measurements
- strong chemisorption interaction (or bond) with Au
- polarity of bond depends on charge on Au
- electrosorption valency shows polar bond at negative charged surface, less so a positive charge surface
- Cl^- is not completely discharged as it is significantly less than one

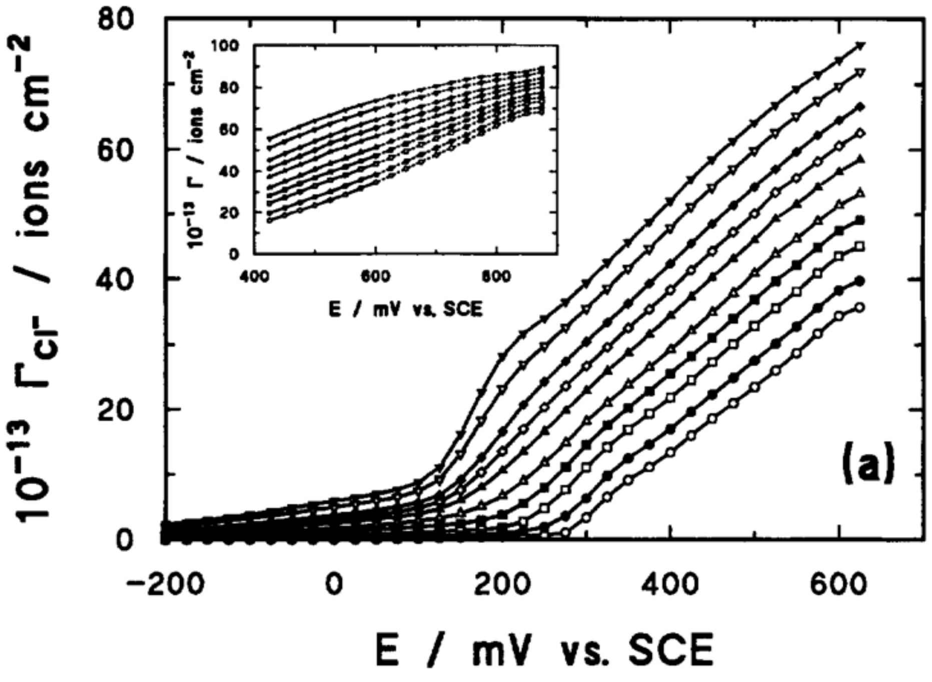

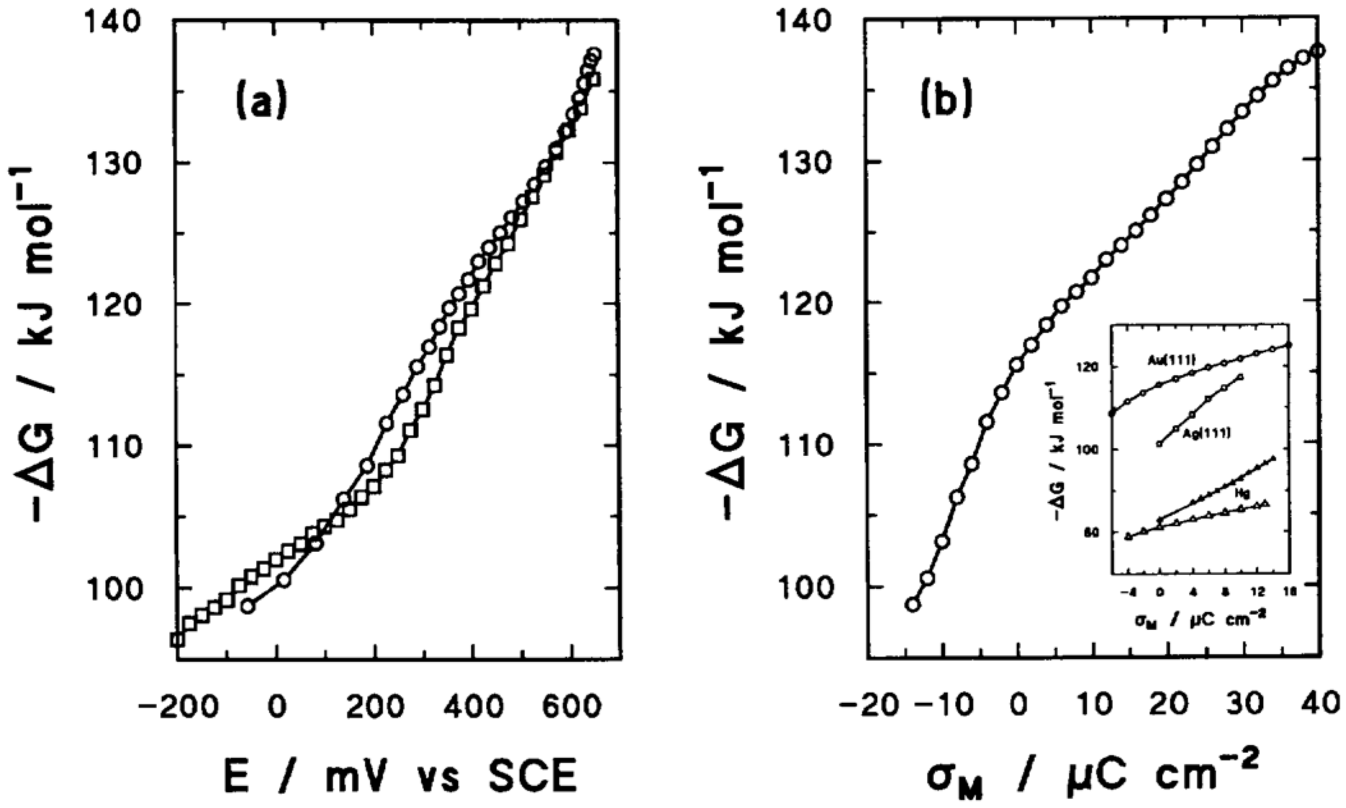

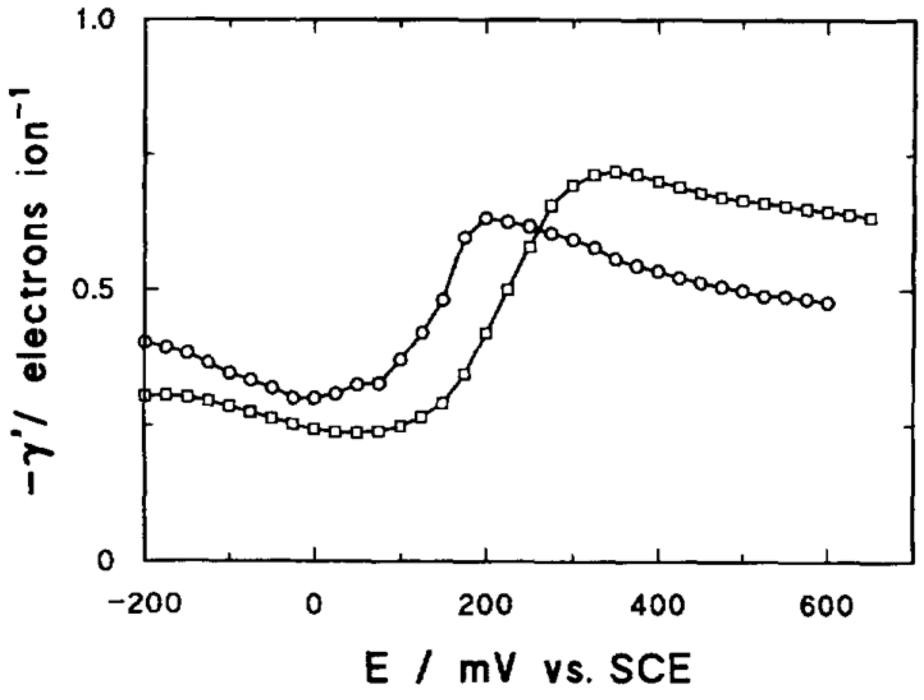

Fig. 9. Electrosorption valencies determined from the slope of the charge versus the Gibbs excess plots (○) and from the Gibbs energy versus electrode potential plots (□).

Shi, Z.; Lipkowski, J. Chloride Adsorption at the Au(111) Electrode Surface. J. Electroanal. Chem. 1996, 403 (1-2), 225–239.

Specific Adsorption on Solid Electrodes

- Cl$^-$, Br$^-$, I$^-$ adsorption on Au(111) compared
- strong chemisorption interaction (or bond) with Au
- polarity of bond depends on charge on Au
- electrosorption valency shows polar bond at negative charged surface, less so on a positive charged surface
- Cl$^-$ is not completely discharged as it is significantly less than one

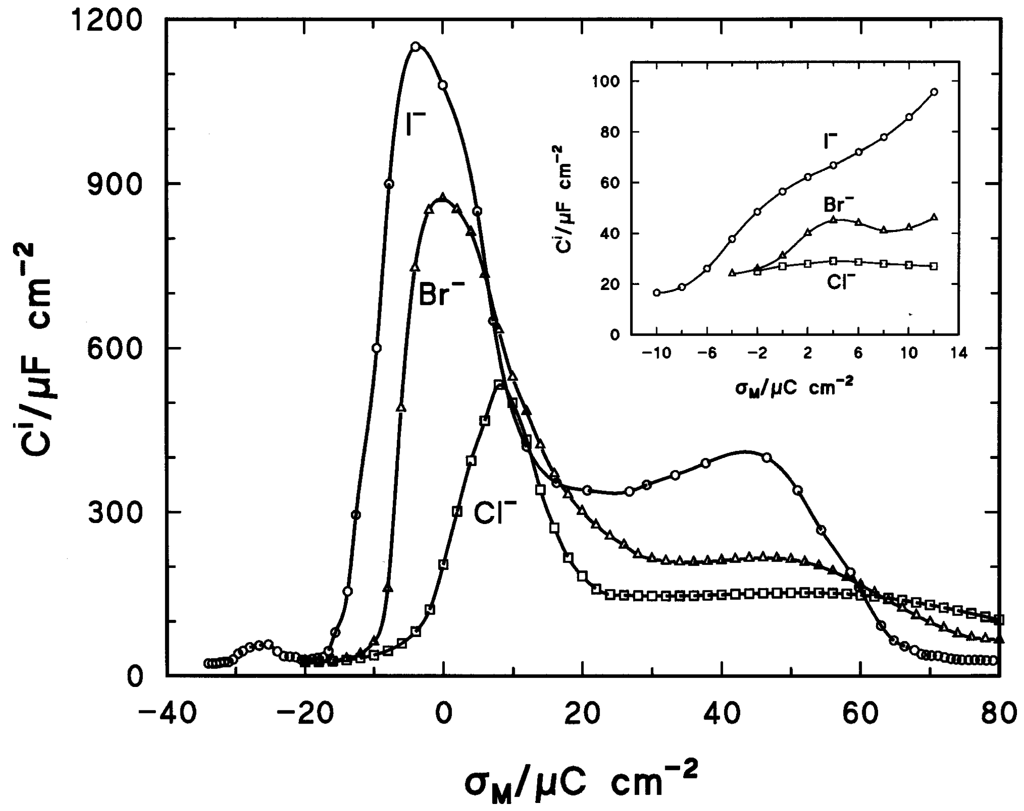

Fig. 10. Comparison of inner layer capacities of the Au(111) electrode for iodide, bromide, and chloride. Inset, comparison of the inner layer capacities of the Hg electrode for the three halides.

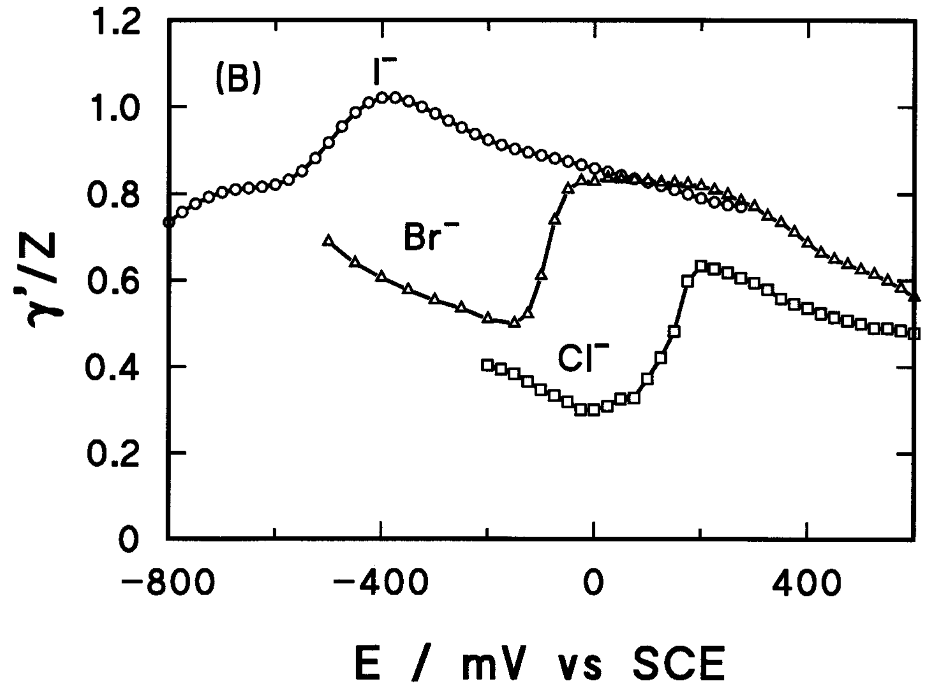

Fig. 8. (A) Electrosorption valences (○) determined from the the charge versus the Gibbs excess plots and (□) from th energy versus electrode potential plots. (B) Comparison of trosorption valences of the three halides.

Chen, A.; Shi, Z.; Bizzotto, D.; Lipkowski, J.; Pettinger, B.; Bilger, C. Iodide Adsorption at the Au(111) Electrode Surface. J. Electroanal. Chem. 1999, 467 (1-2), 342–353.

Specific Adsorption on Solid Electrodes

- comparing Cl$^-$, Br$^-$, I$^-$ adsorption was used to study the inner layer
- inner layer capacity increase correlated with decrease in anion size
- if x_2 is constant, then measuring change in permittivity
- for I$^-$ it is constant: large change in C_i due to solvent reorientation
- Cl$^-$ & Br$^-$: at small charge density, water dipole disordering
- need other measurements to probe interface: spectroscopy

$$\frac{1}{C_i} = \frac{1}{{}_{\sigma}C} - F\left(\frac{\partial \Gamma_I}{\partial \sigma_M}\right)\frac{1}{{}_{\Gamma}C}$$

$${}_{\Gamma}C = \frac{\varepsilon}{(x_2 - x_1)}$$

$${}_{\sigma}C = \frac{\varepsilon}{x_2}$$

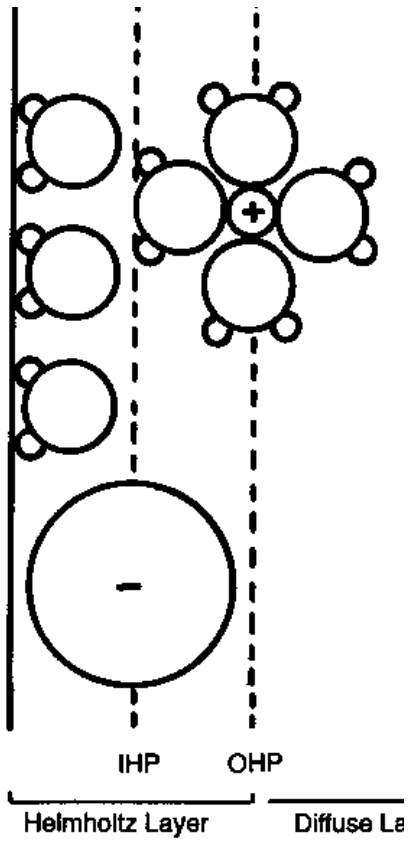

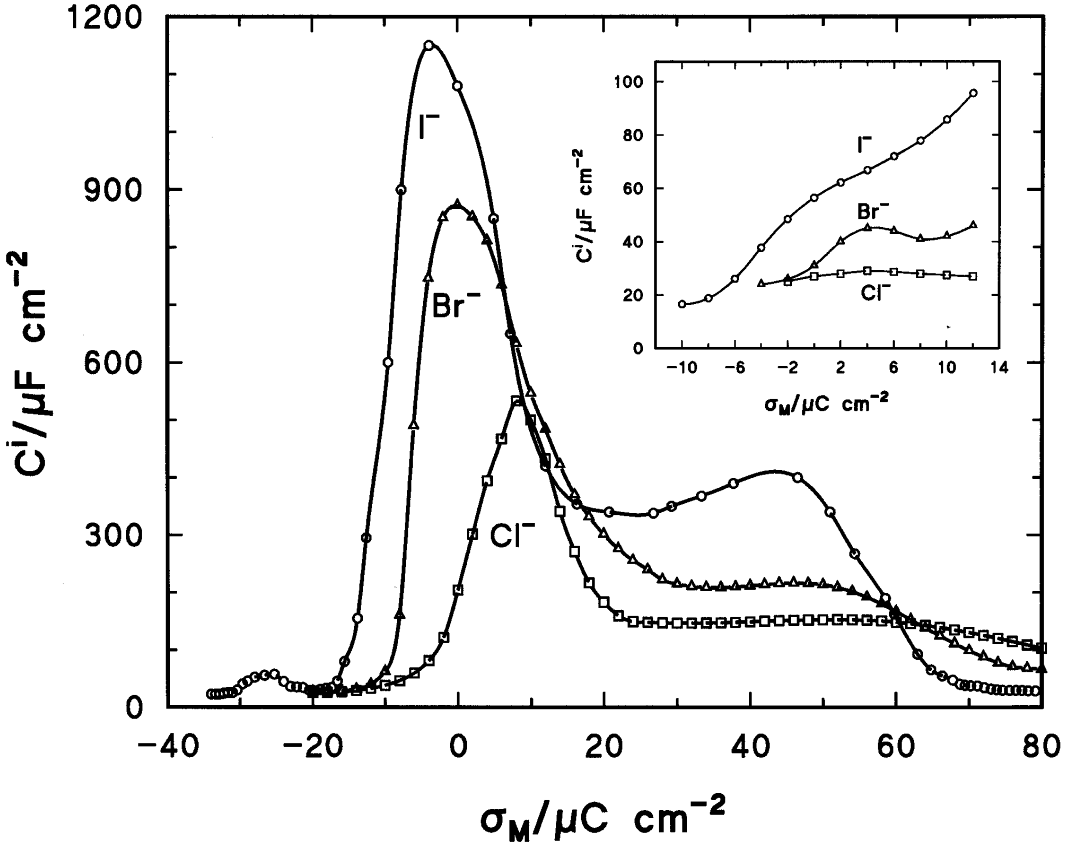

Fig. 10. Comparison of inner layer capacities of the Au(111) electrode for iodide, bromide, and chloride. Inset, comparison of the inner layer capacities of the Hg electrode for the three halides.

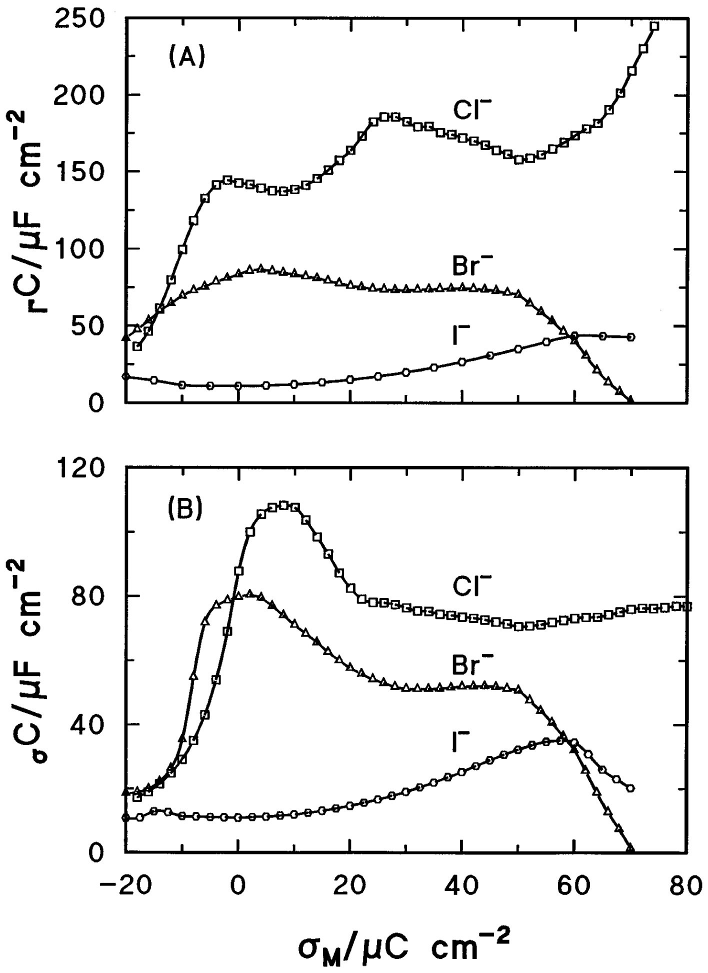

Fig. 12. Comparison of the component of the inner layer capacities for I$^-$, Br$^-$, and Cl$^-$ (A) at constant charge and (B) at constant amount adsorbed.

Chen, A.; Shi, Z.; Bizzotto, D.; Lipkowski, J.; Pettinger, B.; Bilger, C. Iodide Adsorption at the Au(111) Electrode Surface. J. Electroanal. Chem. 1999, 467 (1-2), 342–353.

Specific Adsorption on Solid Electrodes

- electrosorption valency can be estimated from these measurements

$$l = \gamma' = z\left(\frac{{}_{\sigma}C}{{}_{\Gamma}C}\right) = z(x_2 - x_1)/x_2$$

- the metal - surface dipole created between the anion and image charge in metal:

$$\mu_s = z e_o \varepsilon (1 - \gamma'/z)/{}_{\sigma}C$$

- it is a measure of the polarity of the bond

- difficult to determine the distribution of charge in this adsorbed complex - very model dependent
- also an issue in surface modification by physi- or chemi- sorption (eg adsorbed lipids, or alkylthiol SAMs)

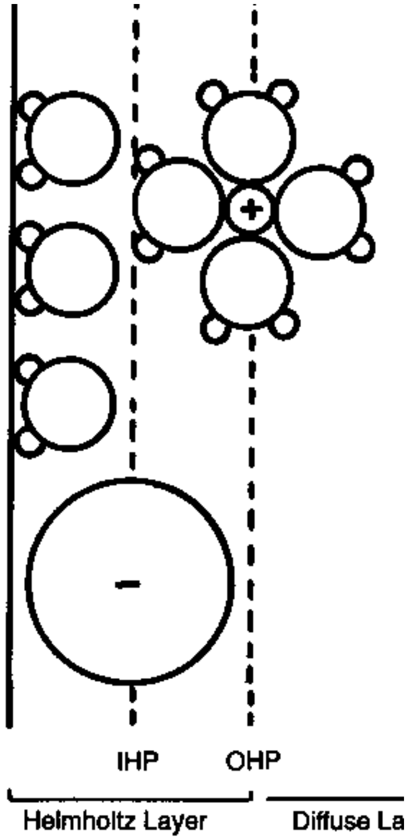

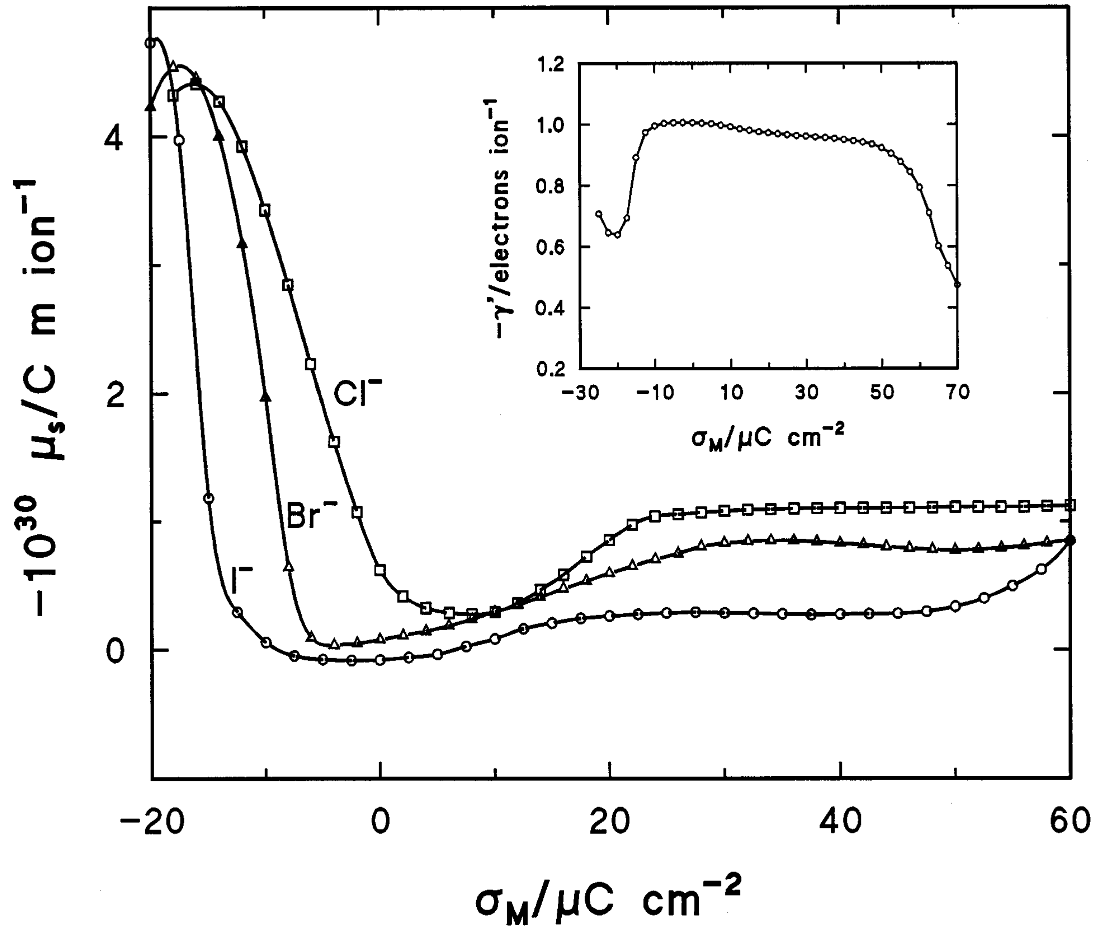

Fig. 13. Plots of the effective dipole moment formed by I^-, Br^-, and Cl^- ion adsorbed at the Au(111) surface versus the charge density on the metal. Inset: electrosorption valency versus electrode charge density plots determined from the ratio of ${}_{\sigma}C$ to ${}_{\Gamma}C$.

Chen, A.; Shi, Z.; Bizzotto, D.; Lipkowski, J.; Pettinger, B.; Bilger, C. Iodide Adsorption at the Au(111) Electrode Surface. J. Electroanal. Chem. 1999, 467 (1-2), 342–353.

Molecular Adsorption

- in real systems, molecular adsorption is typical
- displacement of solvent by adsorbate results in a lower surface tension and capacitance
- for molecules with small dipoles, shift in p.z.c. is small
- desorption (displacement by solvent) occurs at +ve and -ve potentials (w/r to p.z.c.)
- peaks observed in capacitance due to change in coverage:

$$C = \left(\frac{\partial \sigma_M}{\partial E}\right)_\mu = \left(\frac{\partial \sigma_M}{\partial E}\right)_\Gamma + \left(\frac{\partial \sigma_M}{\partial \Gamma}\right)_E \left(\frac{\partial \Gamma}{\partial E}\right)_\mu$$

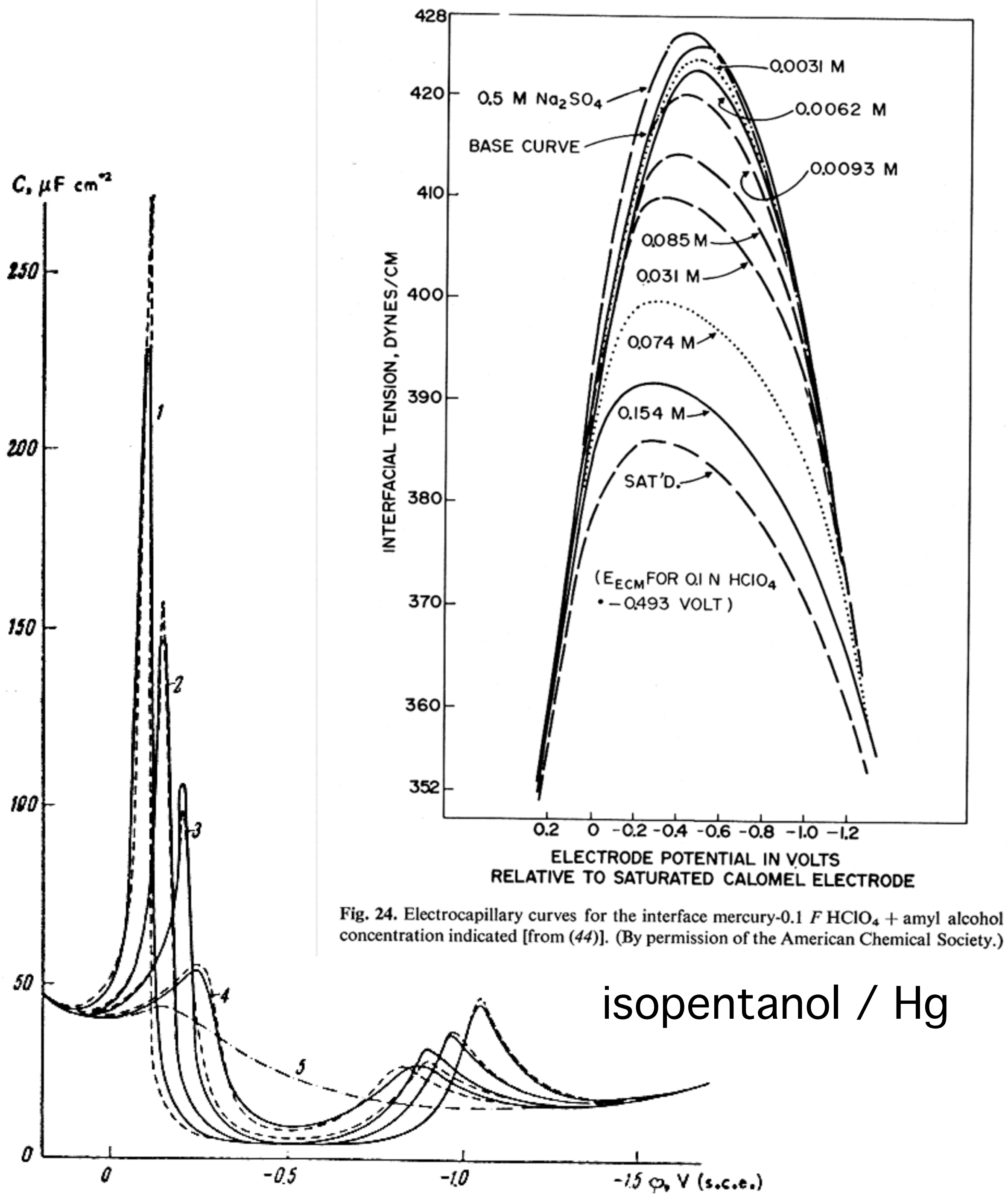

Fig. 24. Electrocapillary curves for the interface mercury-0.1 F $HClO_4$ + amyl alcohol concentration indicated [from (*44*)]. (By permission of the American Chemical Society.)

isopentanol / Hg

Fig. 7. Differential capacitance curves on mercury in 1 N Na_2SO_4 containing different concentrations (M) of isopentanol: 1) 0.04; 2) 0.02; 3) 0.01; 4) 0.005; 5) 0 (pure 1 N Na_2SO_4). The full lines have been calculated by means of Eqn. (1); the broken lines represent experimental data obtained at 450 c/s in the corresponding solutions.

Molecular Adsorption

- composition of the Hg | electrolyte interface can be determined using thermodynamics, model adsorption isotherms
- adsorption free energy, change in dipole due to adsorption, molecular orientation, all as function of electrode charge
- electrosorption valency:

$$-\left(\frac{\partial \Delta G_{ads}}{\partial E}\right)_{\Gamma} = \left(\frac{\partial \sigma_M}{\partial \Gamma}\right)_{E}$$

- interpreted as change in dipole at the interface (using model of inner layer)

$$\left(\frac{\partial \sigma_M}{\partial \Gamma}\right)_{\Delta_2^M \phi} = \Delta_2^M \phi \left(\frac{\partial \frac{\epsilon}{x_2}}{\partial \Gamma}\right) - \frac{\bar{\mu}}{x_2}$$

$$-\partial\gamma = \sigma_M \partial E + \sum_i \Gamma_i \partial \mu_i$$

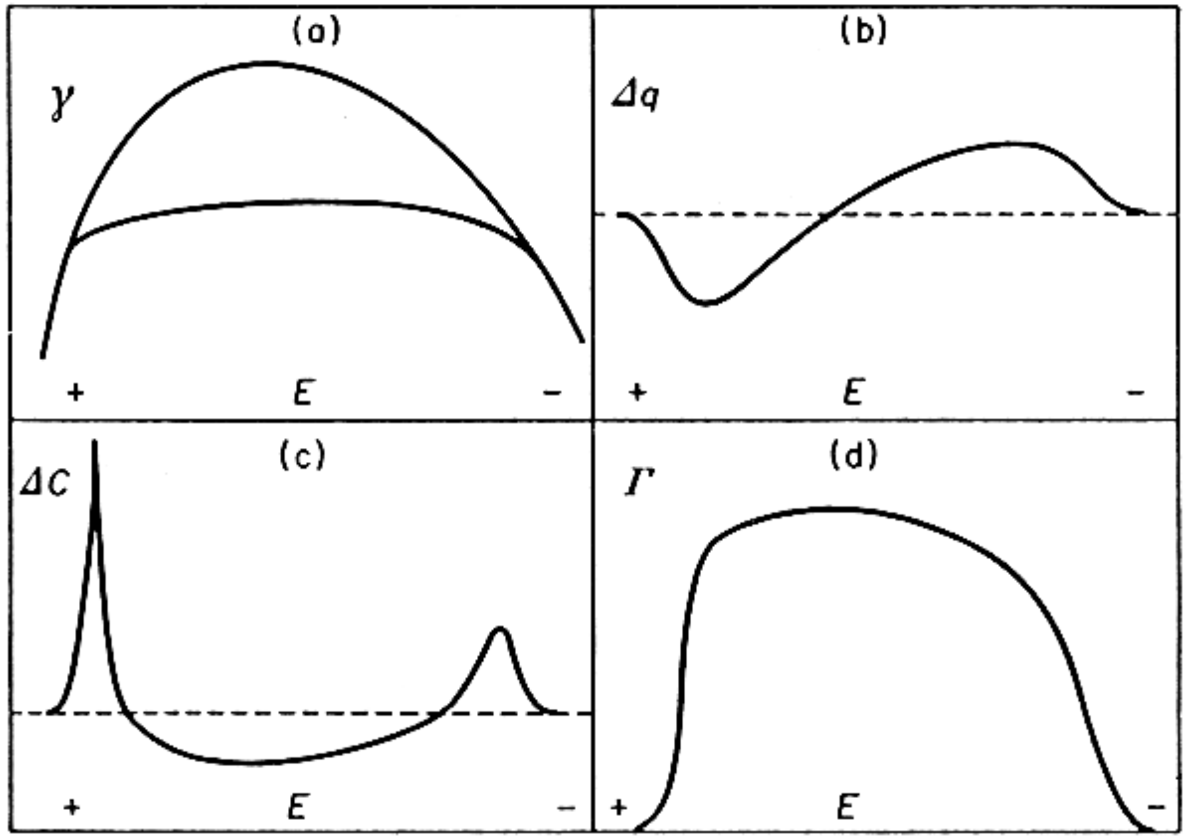

$$\Gamma = \frac{1}{RT}\left(\frac{\partial \pi}{\partial \ln c}\right)_{T,p,E}$$

net change in dipole =
dipole of adsorbate (A) -
dipole of displaced water (W)

$$\bar{\mu} = \bar{\mu}^{A} - n\bar{\mu}^{W}$$

Molecular Adsorption on Solid Electrodes

- As with ionic adsorption, can use the same approach as Hg except measure charge density
- same theory and models used
- amenable to in-situ spectroscopic study

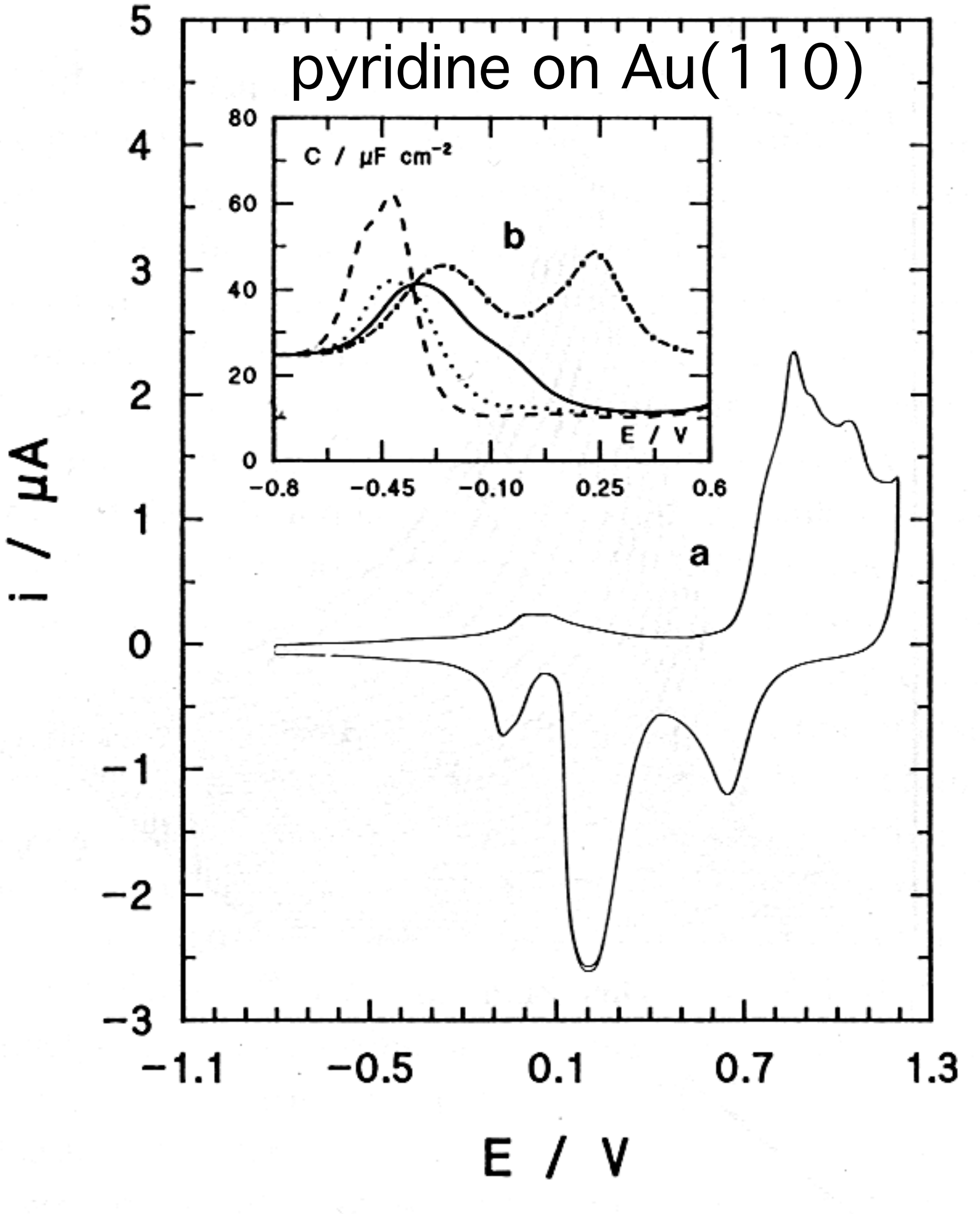
pyridine on Au(110)

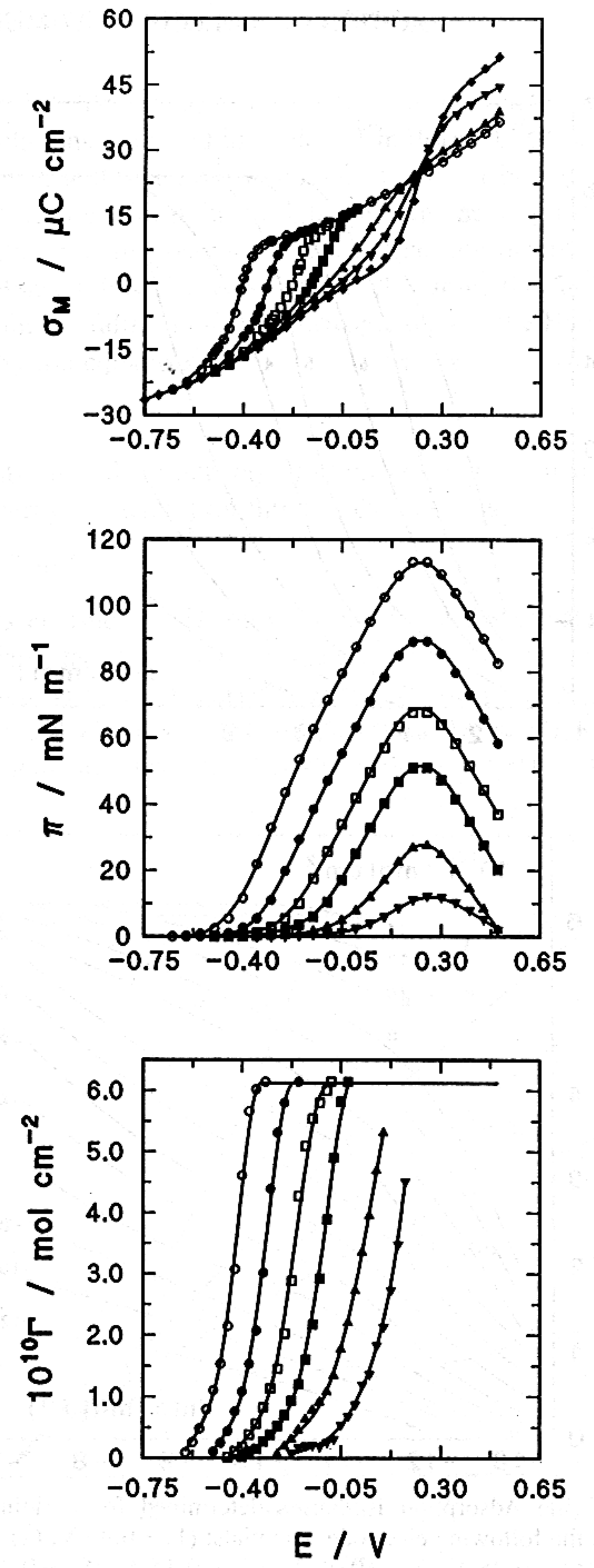

Molecular Adsorption on Solid Electrodes

- pyridine has two orientations on Au:
    - flat lying & standing up with N directed towards the Au
- was determined via shift in p.z.c.
- confirmed with in-situ optical measurements (electroreflectance, IR, Raman)
- many other molecules studied

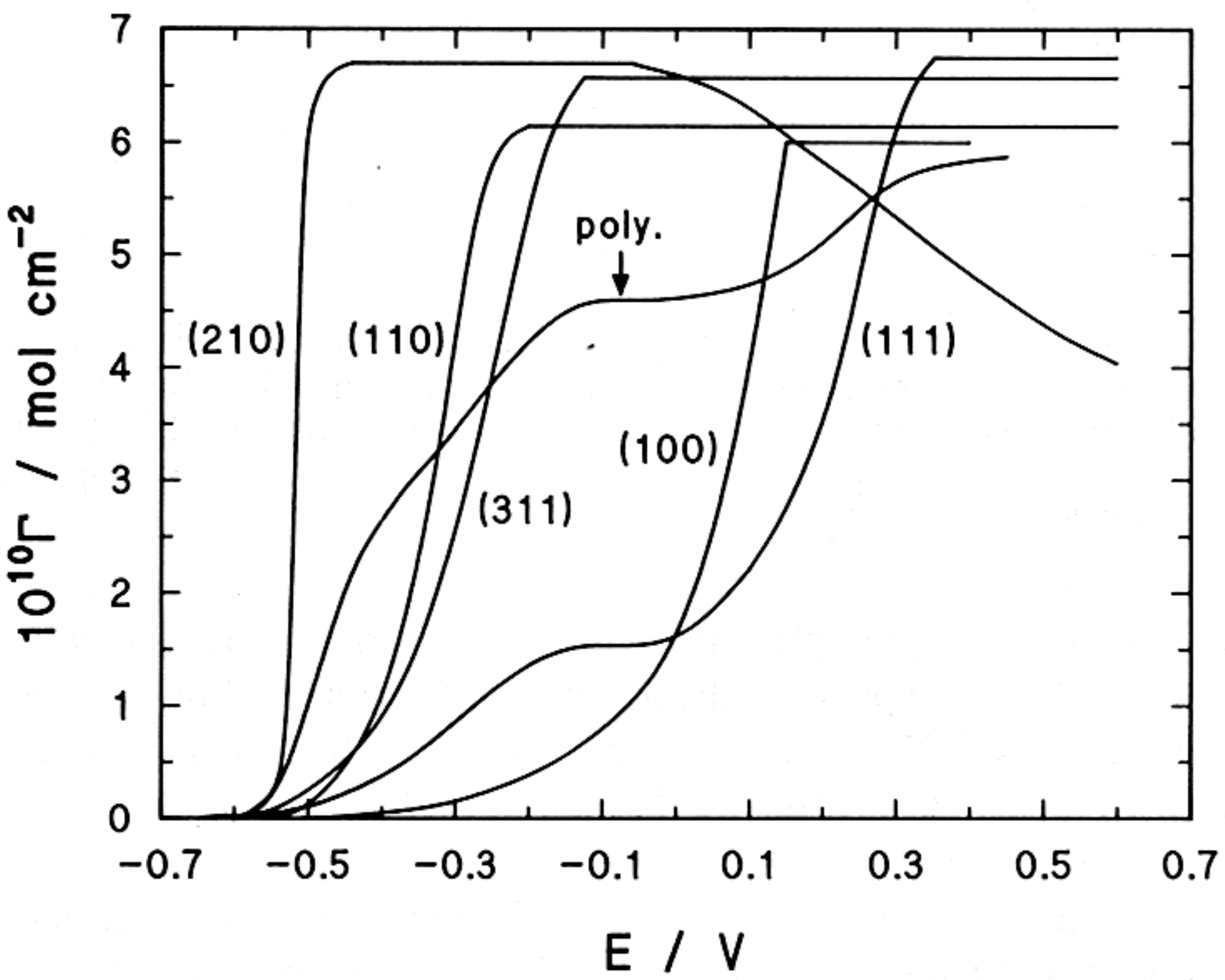

- Thermodymanics has its limits for detailed description of the interface
- need for spectroscopic confirmation, elaboration is clear

in-situ Spectroelectrochemical Methods (SFG)

- thermodynamics cannot provide enough information about molecular orientation without models
- spectroscopy can characterize the metal | electrolyte surface
- Sum Frequency Generation can measure the IR absorption of water from only the surface of the electrode surface.
- Ag(100) and KF :
  - band 2 - strongly H-bonded water
  - band 1 - surface coordinated water
- water orientation at the interface influenced by potential

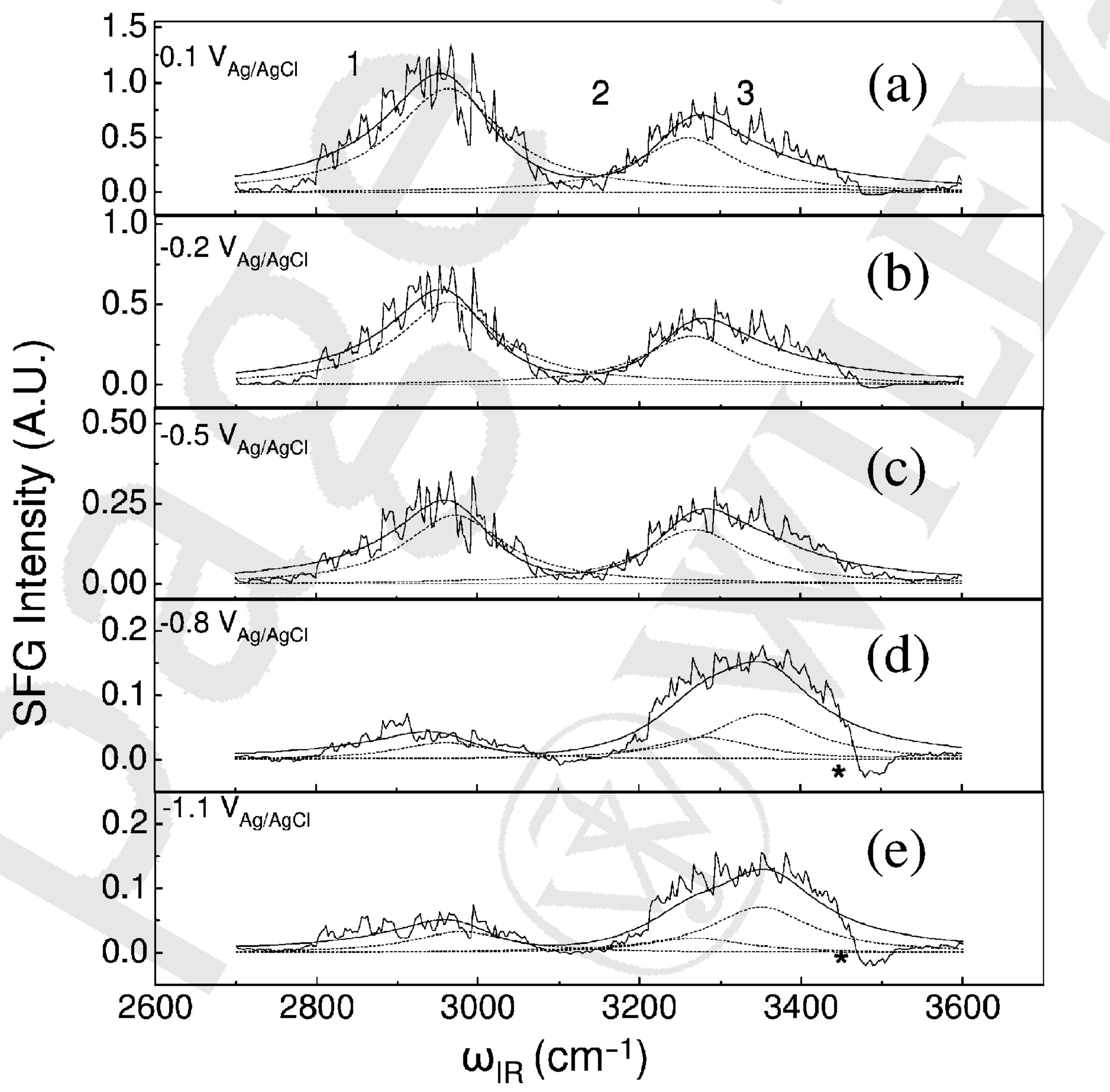

Fig. 5.23 SFG spectra obtained from an Ag(100) surface in 0.1 M KF electrolyte at the applied potentials indicated (a–e). The numbers indicate peak labels as described in the text. Open experimental dat the fitting result the deconvolutio

IR spectroscopy of adsorbed water

- Au(111) in $HClO_4$
- water bands measured using SEIRAS method pioneered by Osawa
- surface sensitive method
- below the p.z.c., H atoms closer to the surface (A)
- changes to (B) flat lying close to p.z.c.
- evidence of ice like water structure on Au around the p.z.c. (C or H)
- ClO_4^- adsorption at positive potentials which changes the water orientation (D)

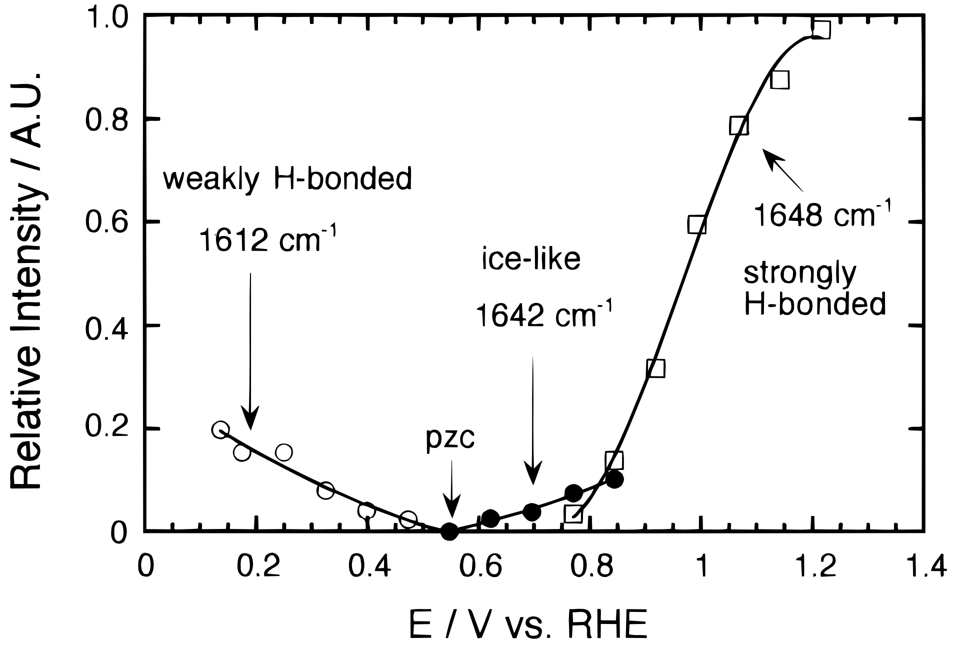

Figure 7. Plot of the integrated intensities of δHOH bands in Figure 4 as a function of applied potential.

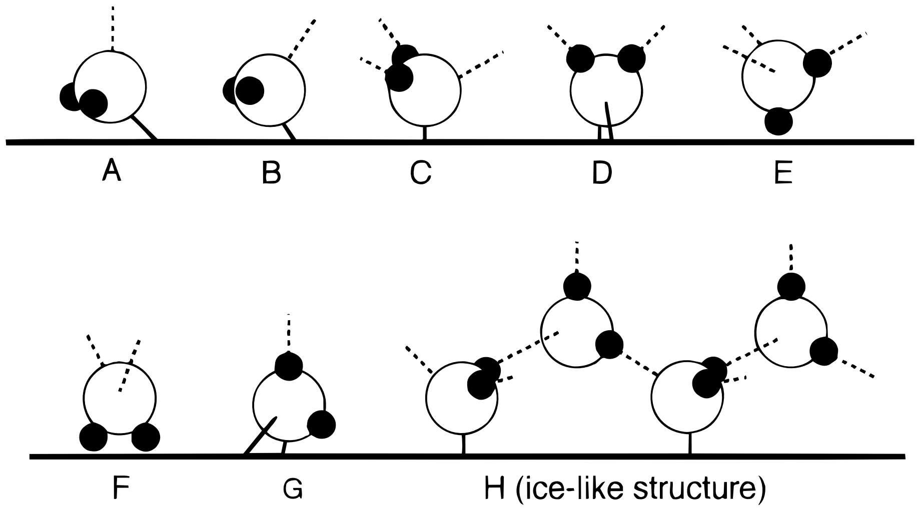

Figure 8. Possible orientations of water at an electrode/electrolyte interface (A−G) proposed in the previous theoretical and experimental studies.[3,9−16,25] The solid lines represent the oxygen lone-pair orbitals interacting with the electrode surface, and the dashed lines hydrogen-bonding (or lone-pair orbitals available for hydrogen-bonding). Model H is an ice-like structure proposed by Doering and Madey.[50] The most plausible orientation deduced in the present study is A at potentials below the pzc, B around the pzc, C slightly above the pzc, and D at more positive potentials.

Ataka, K.-I.; Yotsuyanagi, T.; Osawa, M. Potential-Dependent Reorientation of Water Molecules at an Electrode/Electrolyte Interface Studied by Surface-Enhanced Infrared Absorption Spectroscopy. J. Phys. Chem. 1996, 100 (25), 10664–10672.

Lipid Adsorption on Au: in-situ IR spectroscopy of surface water

- adsorbed lipid bilayer on Au(111)
- lipid is displaced (desorbed) from the Au surface by water at negative potentials
- thin layer of water exists between the electrode and lipid layer (~1-2nm) by insitu neutron reflectivity
- nature of this water studied by surface sensitive FTIR

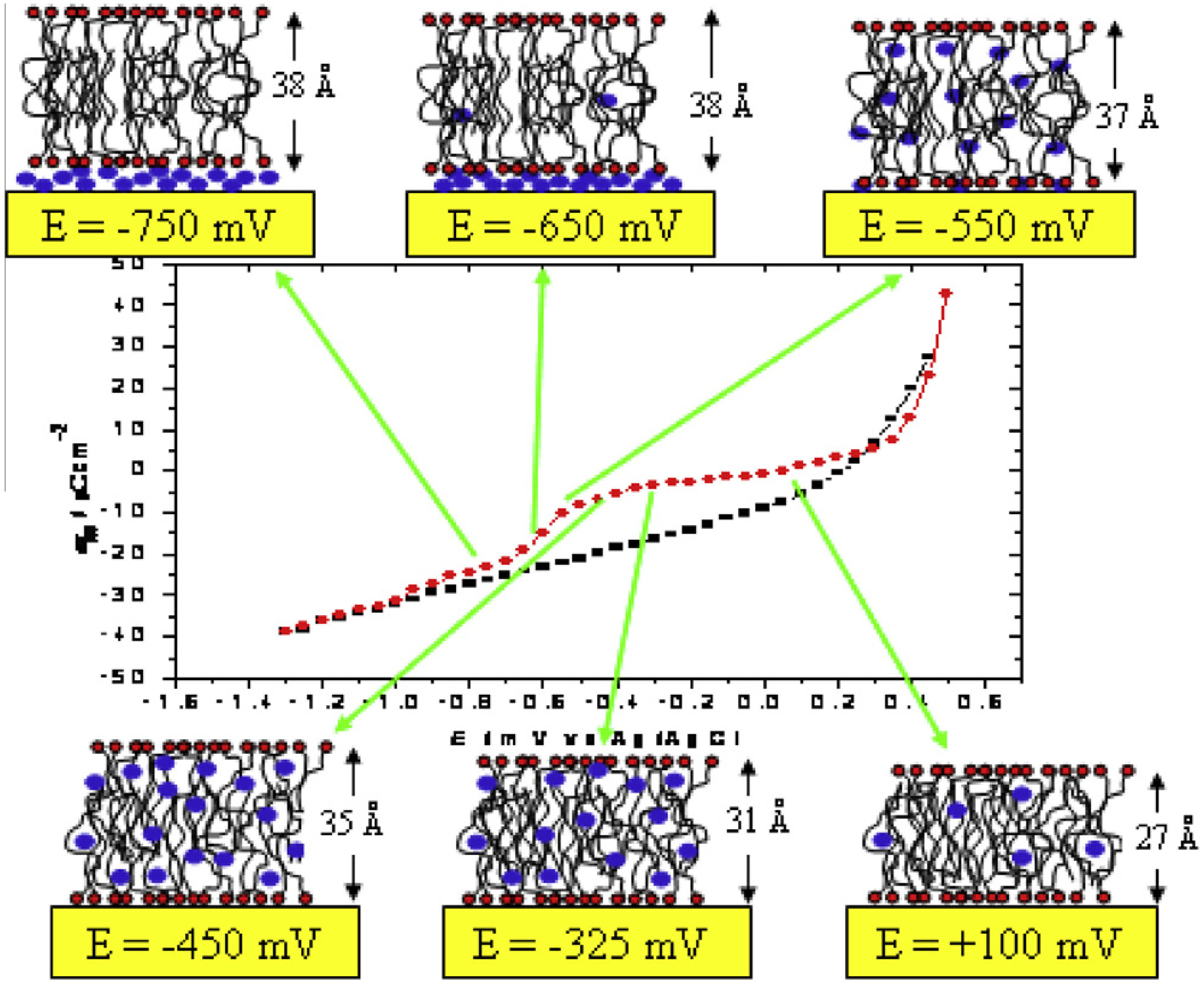

Fig. 1. Pictorial description of the changes in the structure of the mixed DMPC-cholesterol bilayer deposited at the gold electrode surface as a function of the applied potential. The middle section shows charge density curves (black color – 0.05 M NaF supporting electrolyte, red color electrode with the deposited bilayer). Cartoons describe the structure of the bilayer at charge densities indicated in the middle panel by green dots. We emphasize that these cartoons are not models of the biomimetic film but a pictorial description of its structure only. Adapted from Ref. [4]. (For interpretation of the references to color in this figure legend, the reader is referred to the web version of this article.)

Uchida, T.; Osawa, M.; Lipkowski, J. SEIRAS Studies of Water Structure at the Gold Electrode Surface in the Presence of Supported Lipid Bilayer. J. Electroanal. Chem. 2014, 716, 112–119.

Lipid on Au: Interfacial water

- probing both stretching and bending of HOH
- 3600cm^{-1} multimer water
- 3400 & 3250cm^{-1} network water
- ratio of water type depends on potential
- (E > -0.5V) when adsorbed, the water is similar to multimer water: broken network of H-bonds
- (E < -0.5V) when desorbed, water is not free, bound to lipid head groups, but more perturbed than for hydrated lipid bilayer

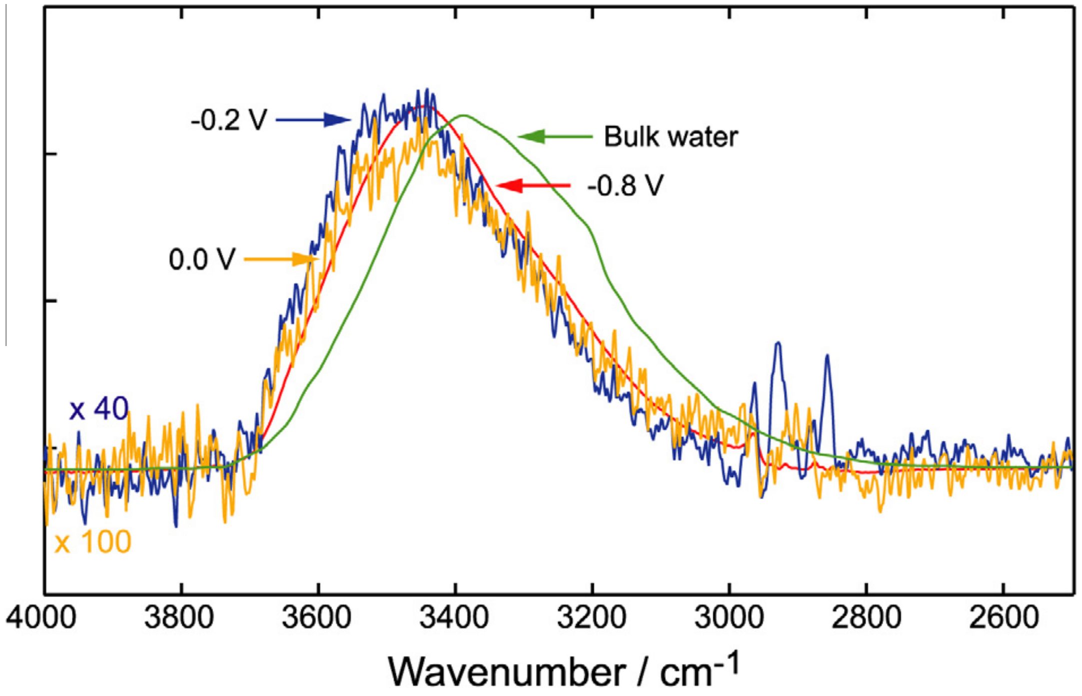

Fig. 6. Comparison of SEIRA spectra: (red line) taken at –0.8 V; (blue line) taken at –0.2 V; (yellow line) taken at 0.0 V; (green line) transmission IR spectrum of bulk water. (For interpretation of the references to color in this figure legend, the reader is referred to the web version of this article.)

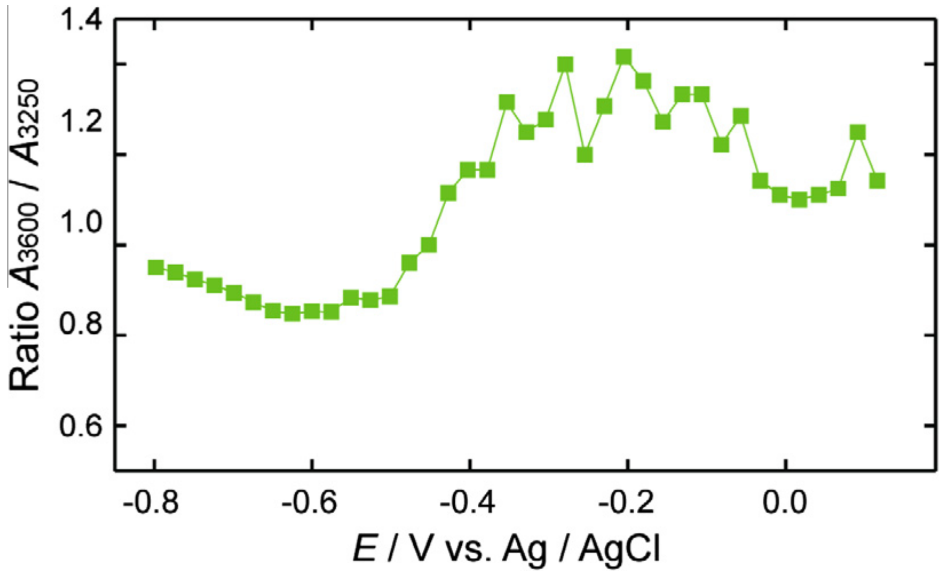

Fig. 7. Absorbance ratio of the ν(OH) subbands at 3600 and 3250 cm^{-1} plotted as a function of the applied potential.

Lipid on Au: Interfacial water

- study bending of HOH
- 1595 cm^{-1}: isolated water in gas phase
- 1645 cm^{-1}: liquid water
- 1670 cm^{-1}: amorphous ice
- for E < -0.6V:
    - layer of water is developing ,
    - little isolated water,
    - hydrogen bonding network, but perturbed due to metal surface & potential
- at E = -0.8V, similar to bulk water, but less ordered

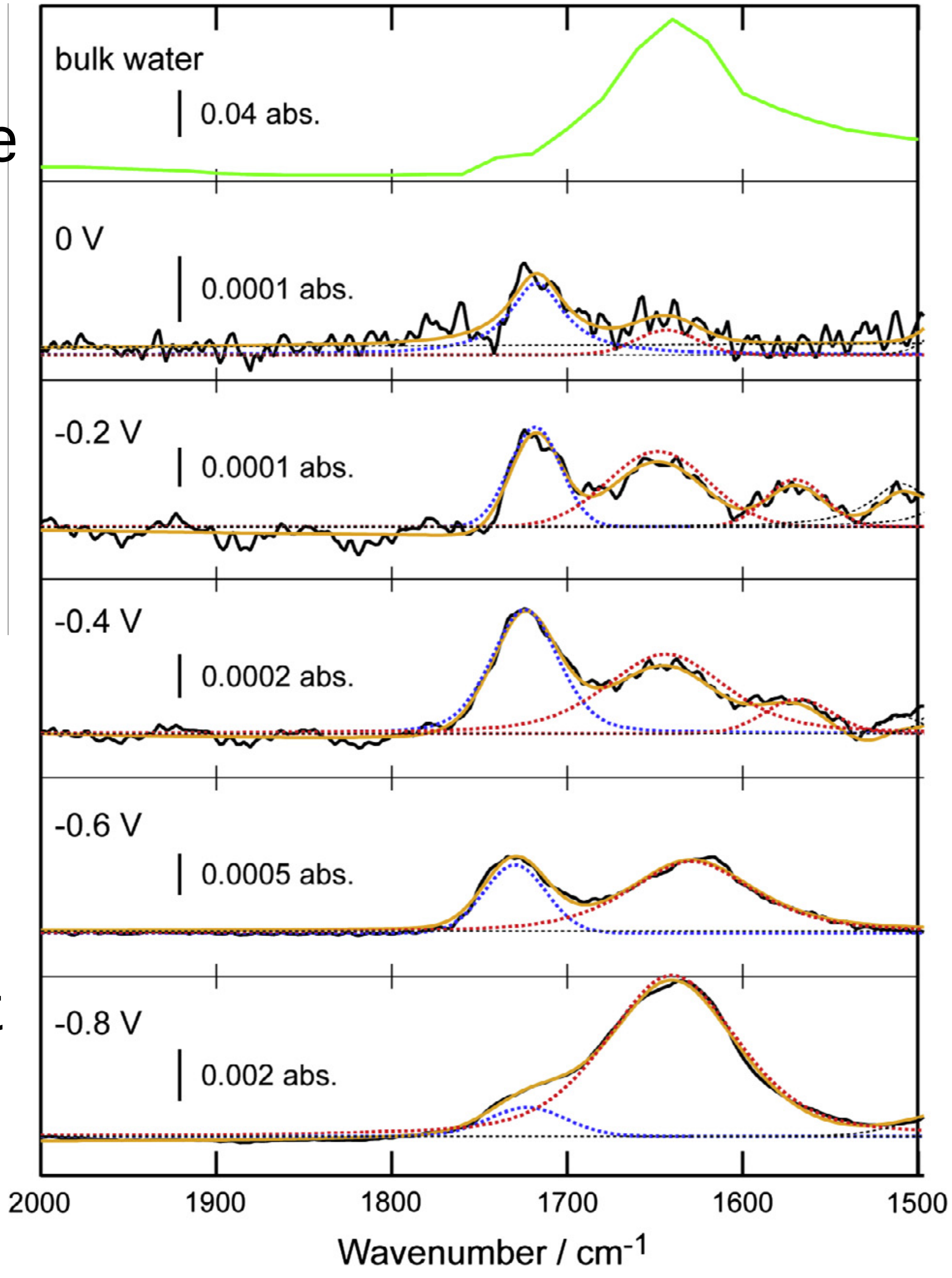

Fig. 8. Comparison of SEIRA spectra in the δ(HOH) band spectral region at selected potentials to the transmission IR spectrum of water.

EIS Evidence of structured water at interface

- DOPC lipid monolayer adsorbed onto Hg
- potential driven phase changes
- displacement by electrolyte at negative charge densities (-1.8V/SCE)

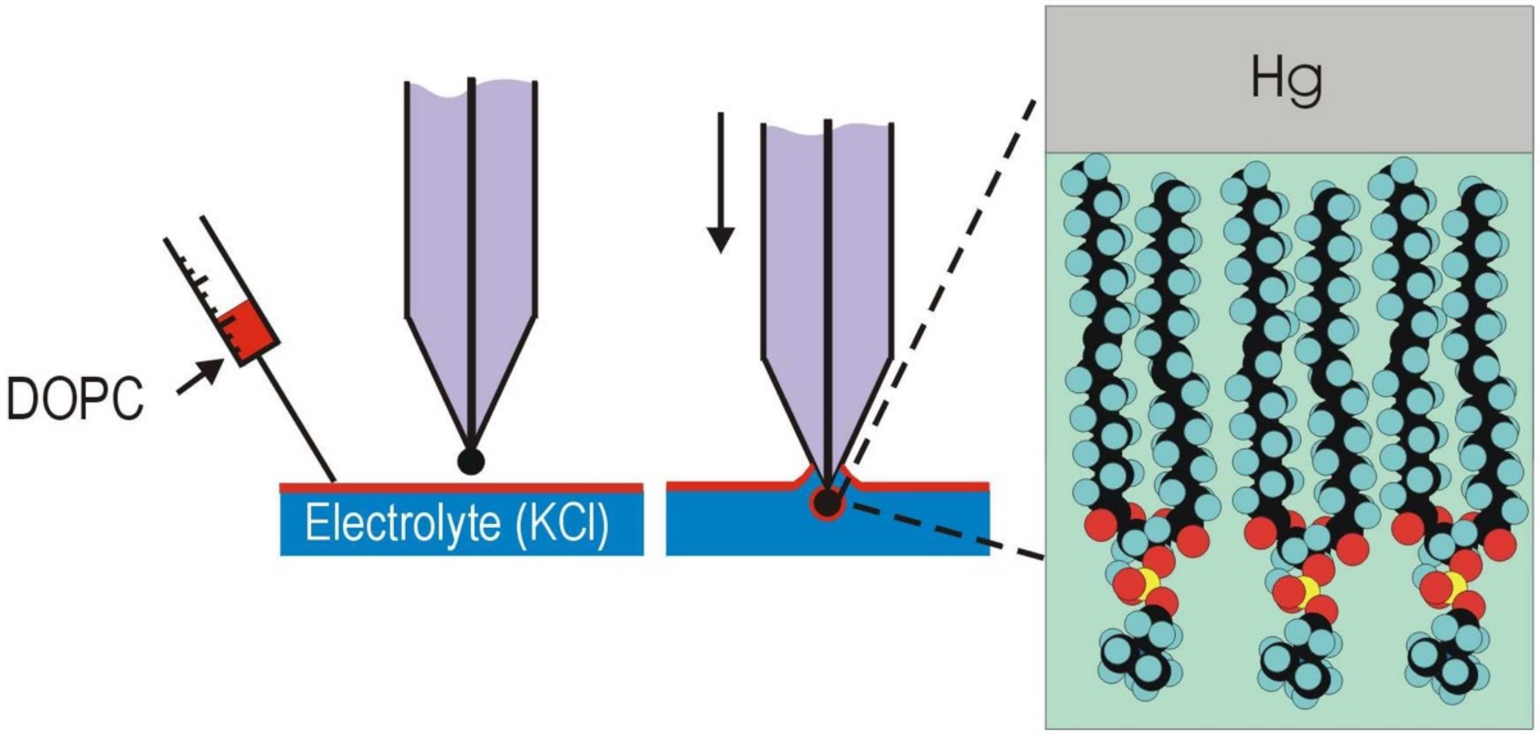

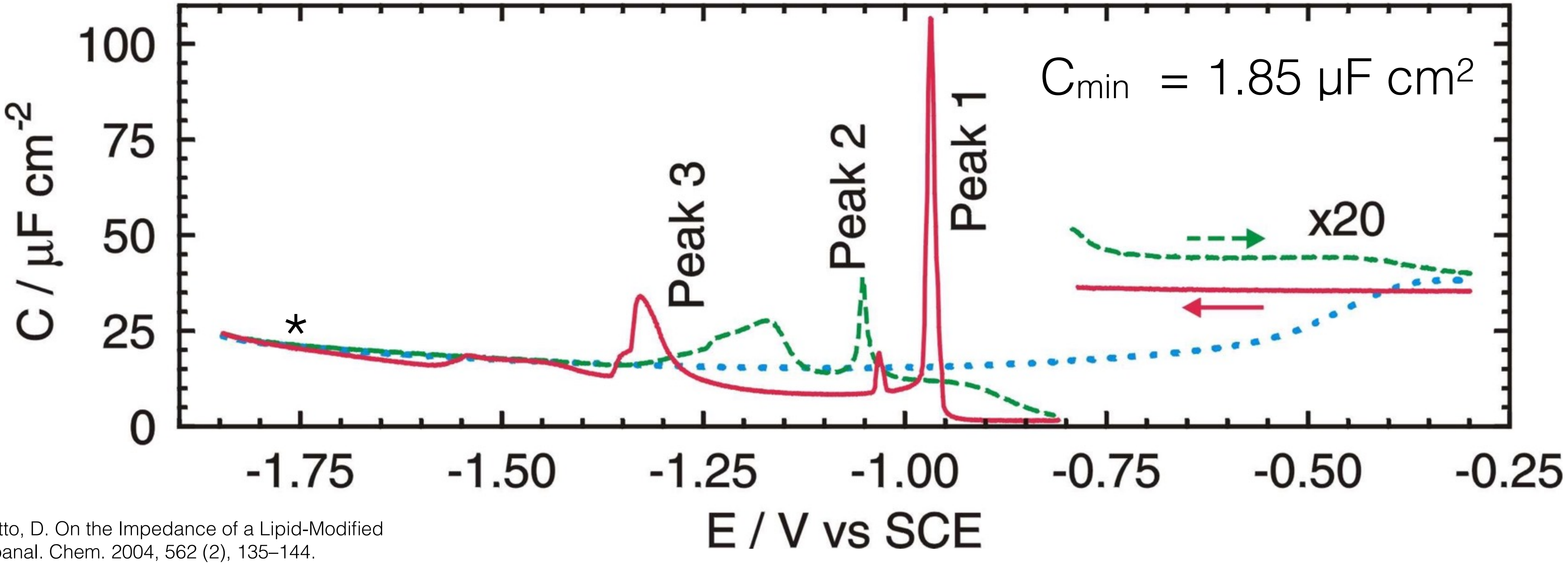

Agak, J. O.; Stoodley, R.; Retter, U.; Bizzotto, D. On the Impedance of a Lipid-Modified Hg|Electrolyte Interface. J. Electroanal. Chem. 2004, 562 (2), 135–144.

DOPC monolayer from Liposomes

- can form the monolayer from liposomes
- differences in potential dependent capacitance behaviour observed
- EIS at -1.85V/SCE

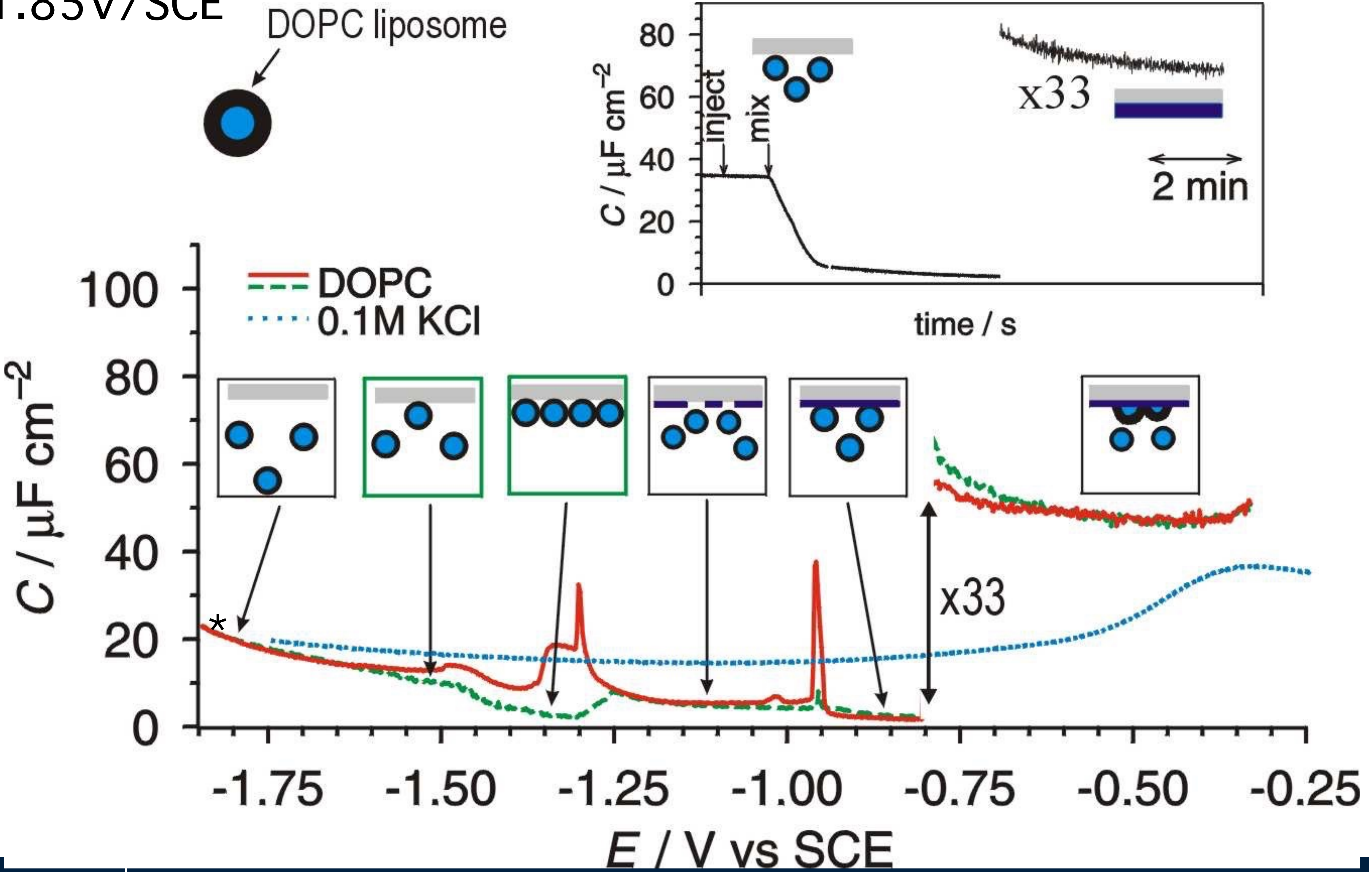

- EIS on Hg | lipid at desorption potentials
- thin layer of water present between the lipid and Hg
- extra elements needed to model desorbed liposome layer
- represent a change in water exchange on electrode
- lipid near electrode (not adsorbed) tends to influence water order

water relaxation:
liquid: < ns
ice: 10μs
adsorbed: 1ms - 1 μs

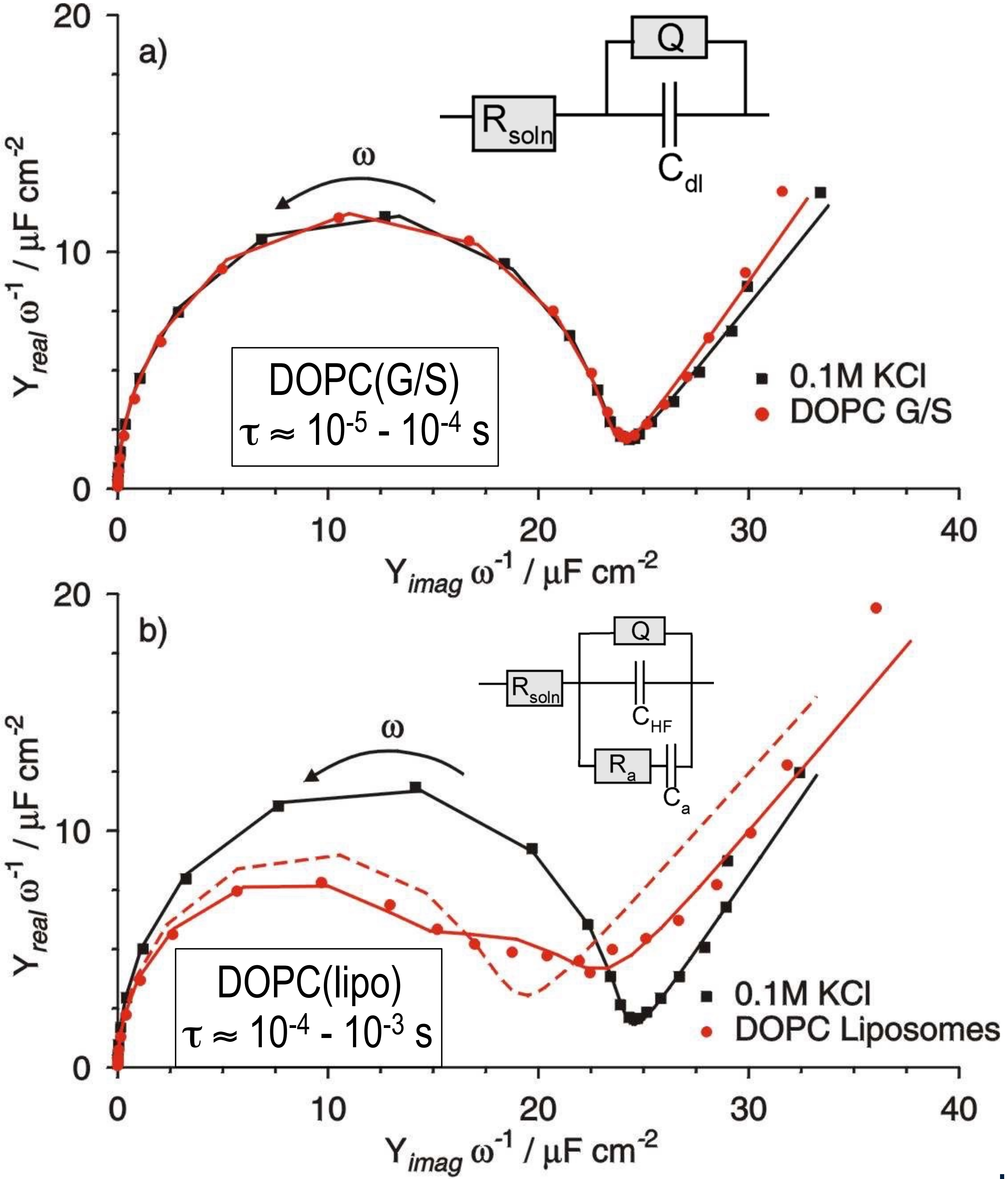

Complex Electrochemical Interfaces

- metal electrodes are easily modified via alkylthiol monolayers
- introduce a variety of surface functionalities that have charge
    - eg: acids, amines, peptides, nucleic acids

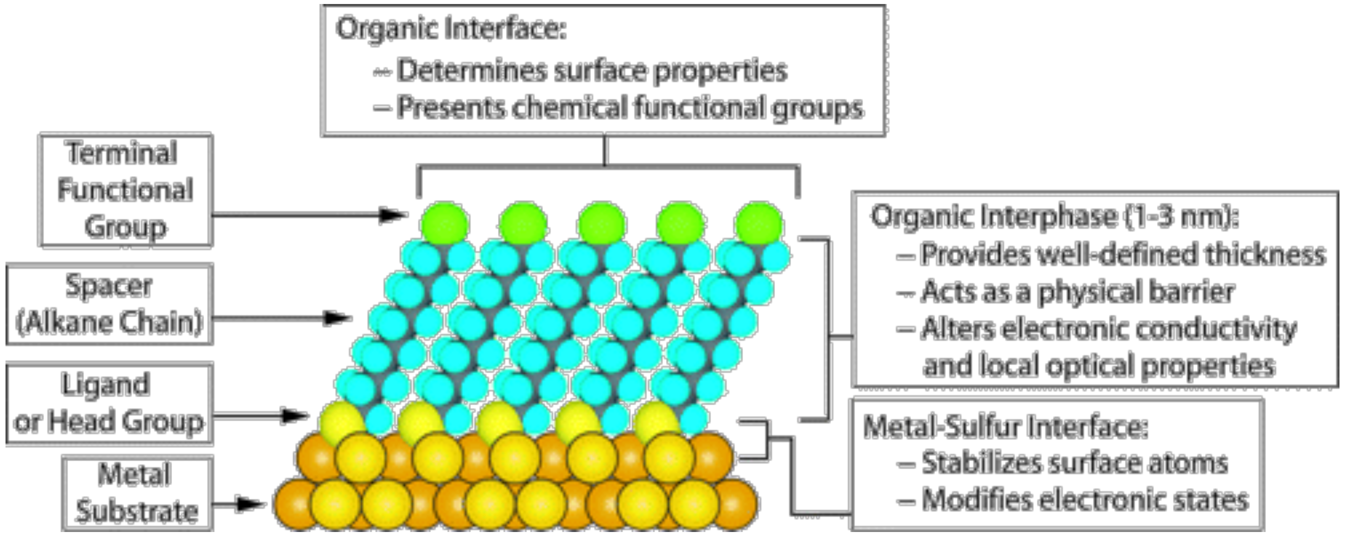

- challenge is to create consistent high quality interfaces

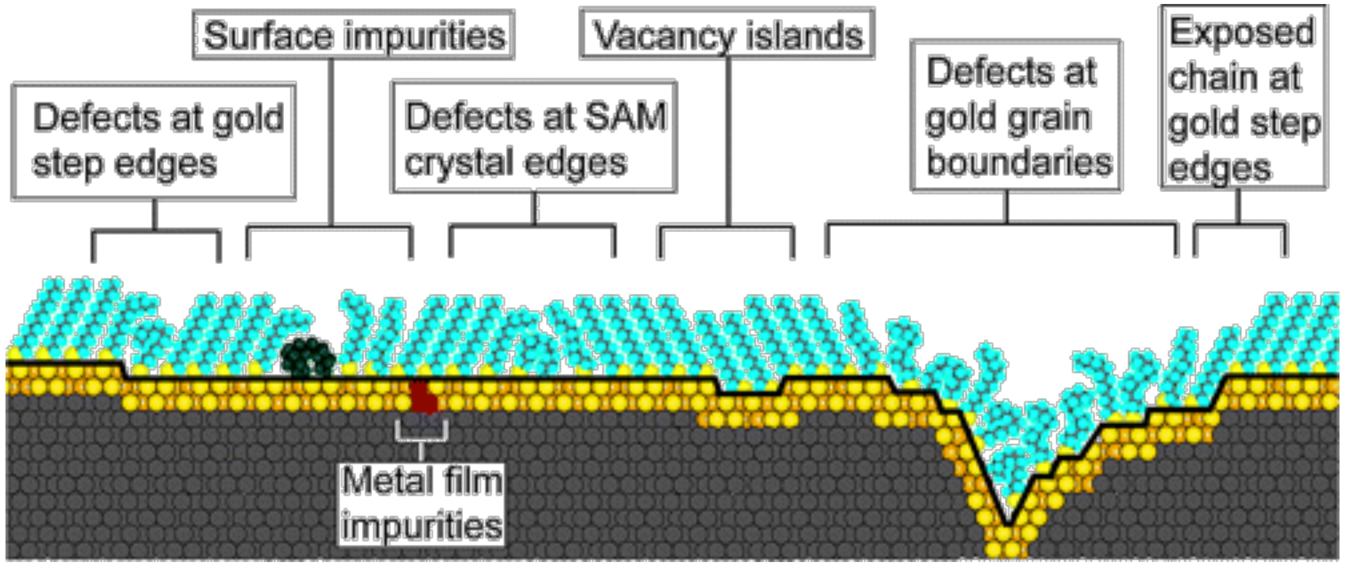

Love, J. C.; Estroff, L. A.; Kriebel, J. K.; Nuzzo, R. G.; Whitesides, G. M. Chem. Rev. 2005, 105, 1103–1169.

Interesting Experimental Systems

- modified electrode surfaces with charged molecules
- SAM of MUA shows peaks at pH ~ pKa
- maximum in capacitance with pH

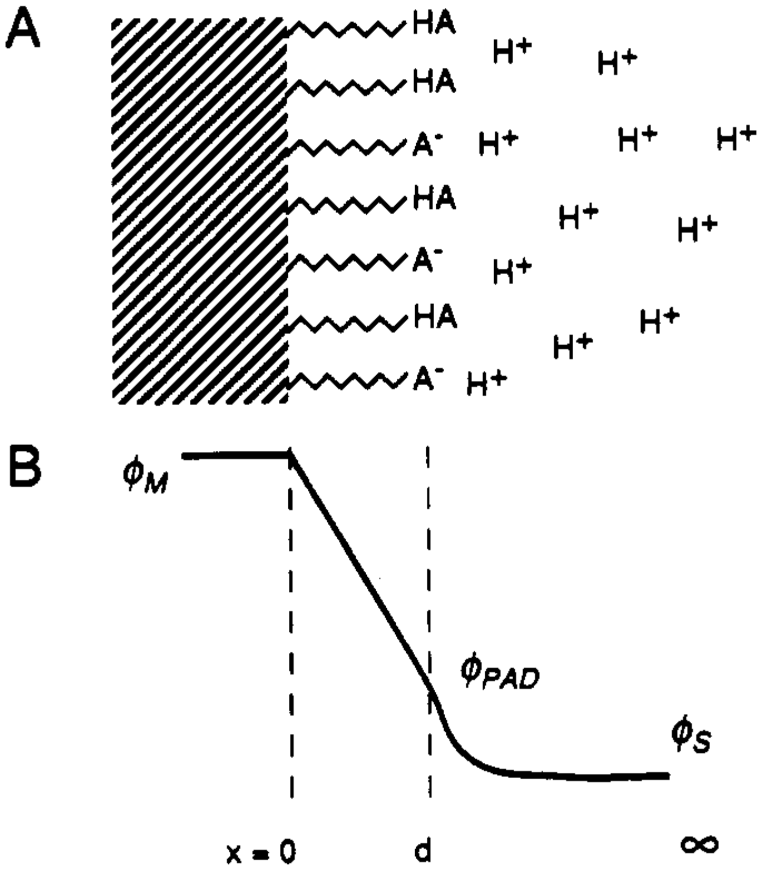

Figure 1. (A) Schematic representation of an adsorbed monolayer of an acid/base pair in contact with an electrolyte solution. (B) Variation of potential from the electrode surface to the bulk of the solution. The acid/base groups of all the molecules are assumed to lie in a common plane, the "plane of acid dissociation" (PAD), located a distance *d* from the electrode surface.

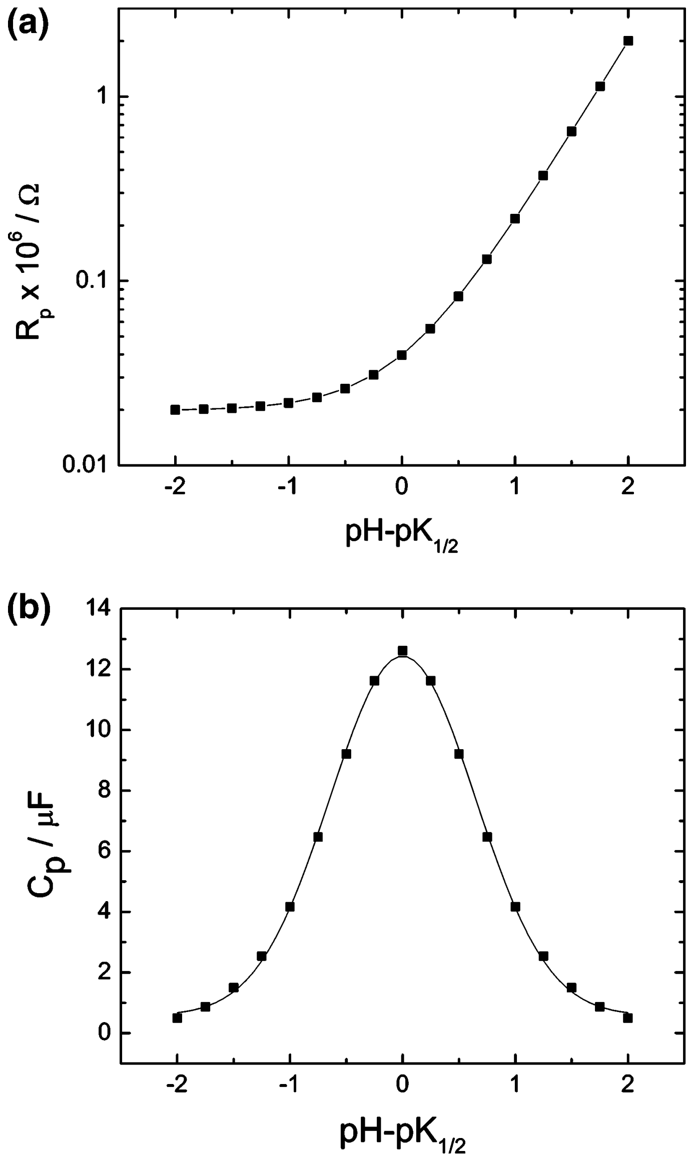

Figure 6. Simulated values of R_p (a) and C_p (b) vs pH for potentials corresponding to the maximum protonation/deprotonation current.

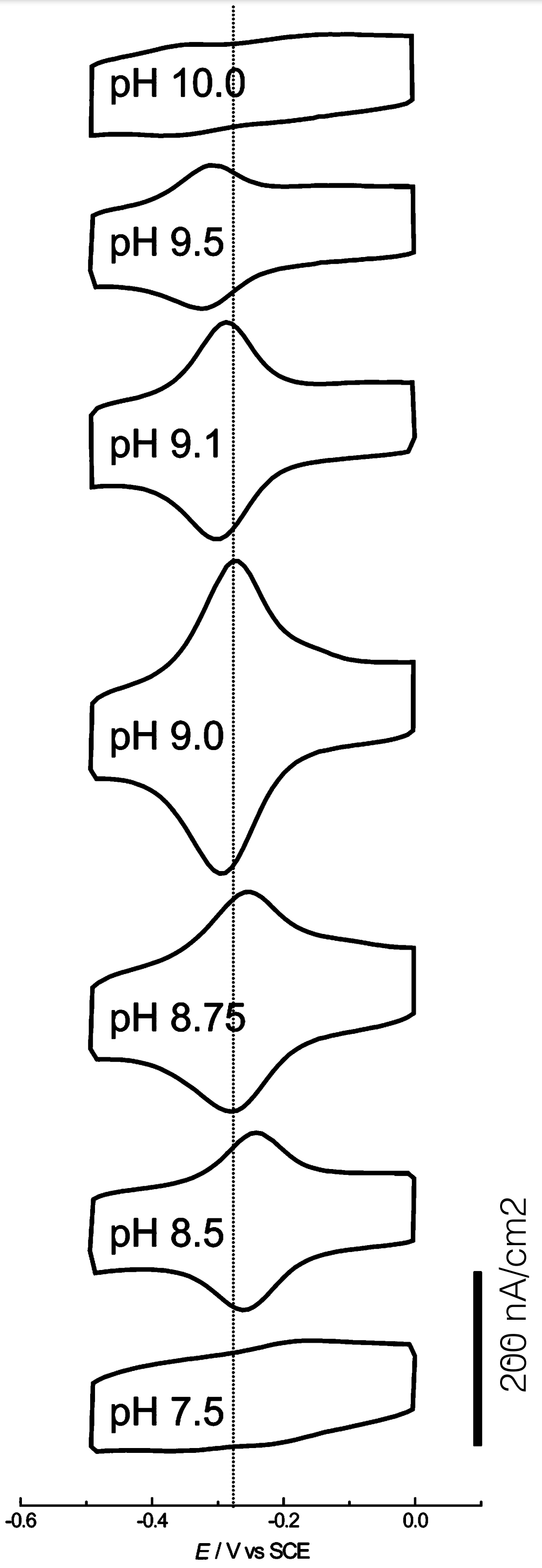

Smith, C. P.; White, H. S. Voltammetry of Molecular Films Containing Acid/Base Groups. Langmuir 1993, 9 (1), 1–3.
Burgess, I.; Seivewright, B.; Lennox, R. B. Electric Field Driven Protonation/Deprotonation of Self-Assembled Monolayers of Acid-Terminated Thiols. *Langmuir* **2006**, *22* (9), 4420–4428.

Interesting Experimental Systems: DNA SAMs

- modified electrode surfaces with polyelectrolytes like DNA
- nature of the EDL with fixed charges
- potential drop can change orientation of the DNA
- strong influence of electrolyte concentration - influences the screening
- hybridization on surface and EDL influence - impact on DNA sensors

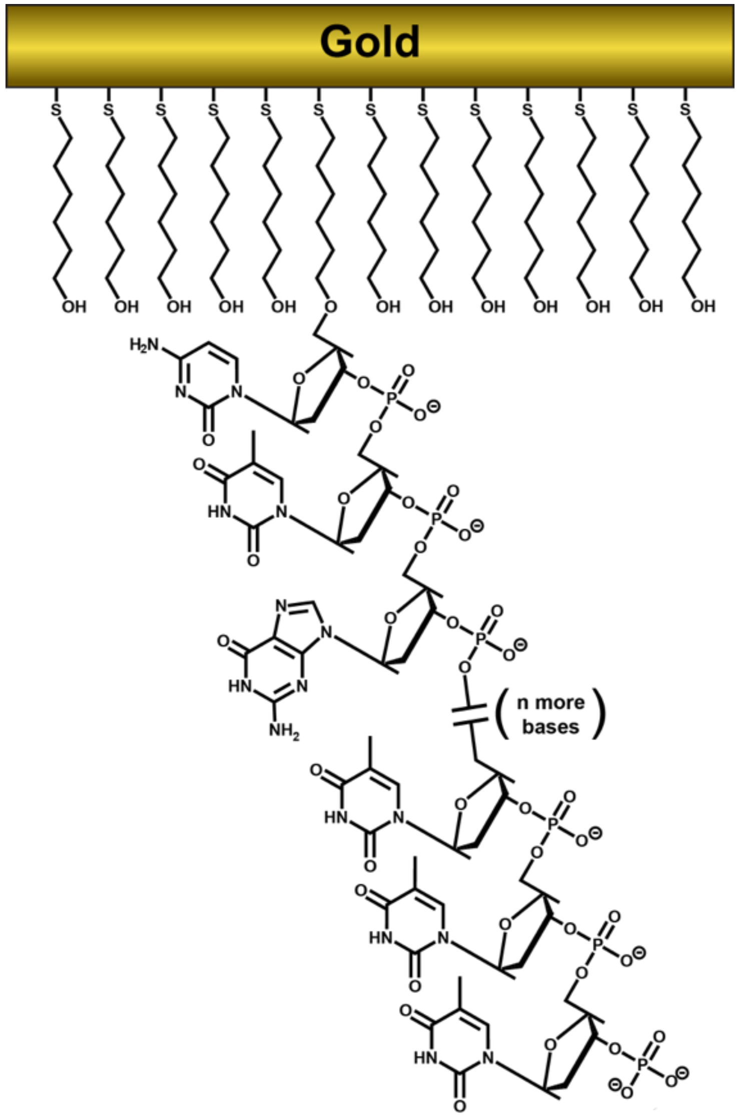

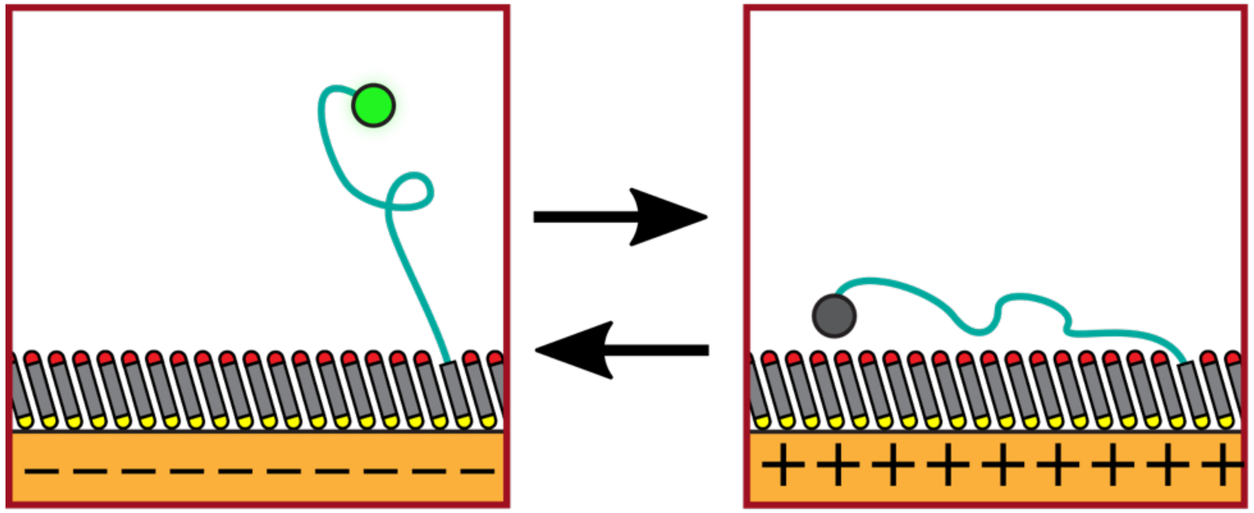

Interesting Experimental Systems: DNA SAMs

- mixed monolayer: MCH & DNA modified electrode surfaces
- interacts with potential gradient normal to the surface
- experiments show orientation of adsorbate depends on potential
- rate of reorientation depends on size & rigidity of adsorbed DNA
- DNA is polyelectrolyte, brings significant charge density into the inner - diffuse layer region

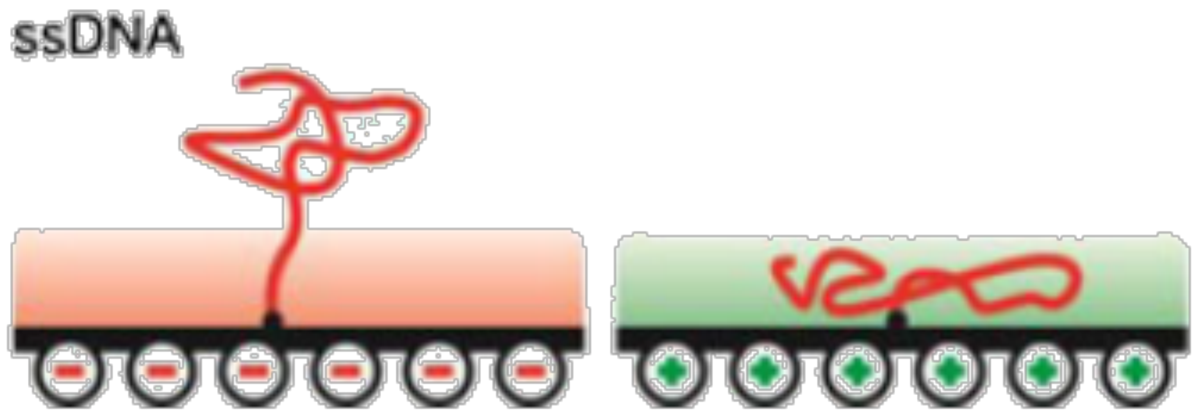

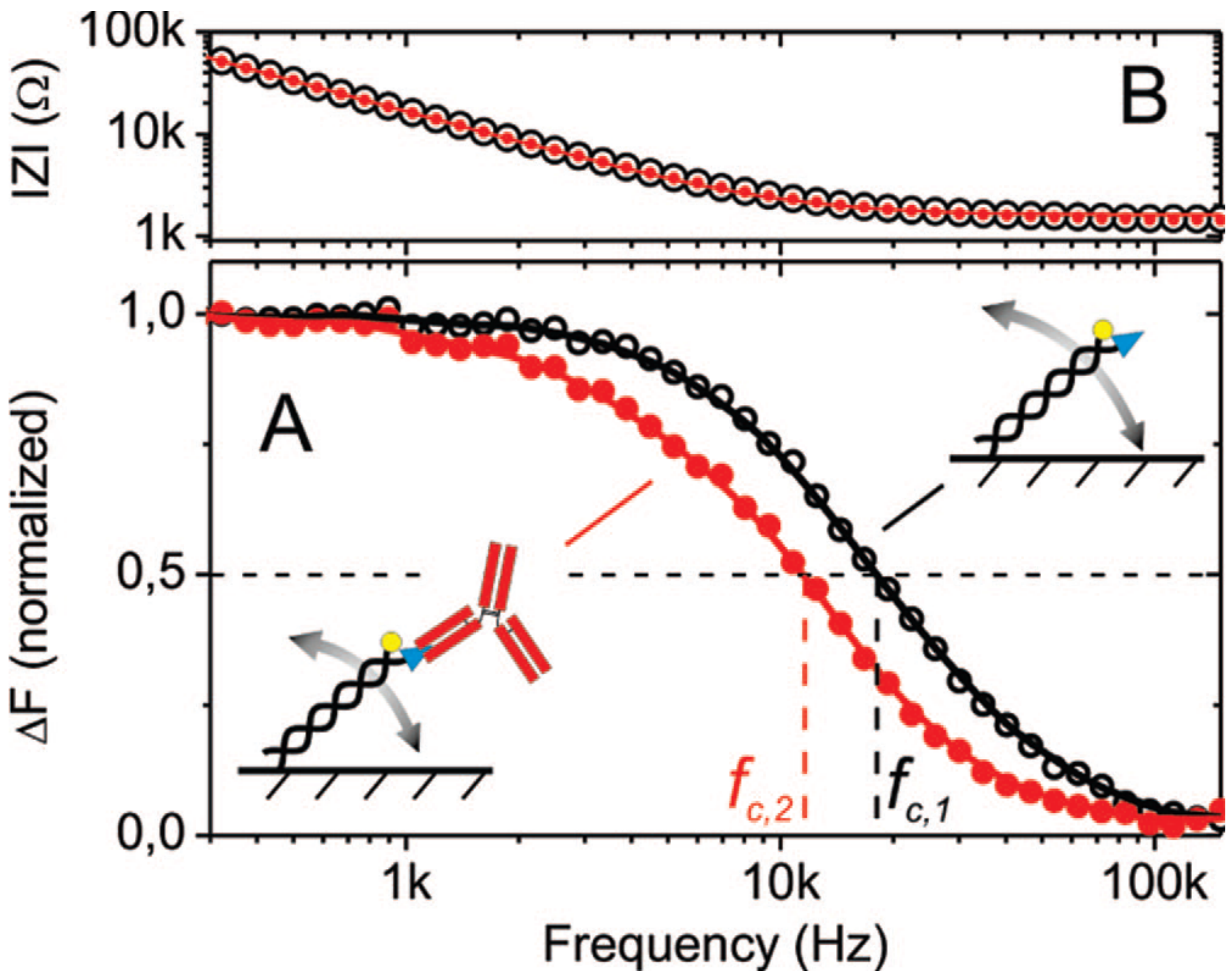

Rant, U et al. Nano Letters 2009, 9, 1290–1295

Interesting Experimental Systems

- electrostatic field needs to interact with the tethered DNA to influence its orientation
- high ionic strength: dsDNA rapidly changes orientation; ssDNA is compact
- medium ionic strength: dsDNA - ~ 5bp in strong electric field; ssDNA - flexible & more mobility
- low ionic strength: dsDNA is not stable; ssDNA extends becomes rod -like due to increase in electrostatic persistence length in low ionic strength
- GCS used to calc potential drop, what is the influence of the polyelectrolyte?

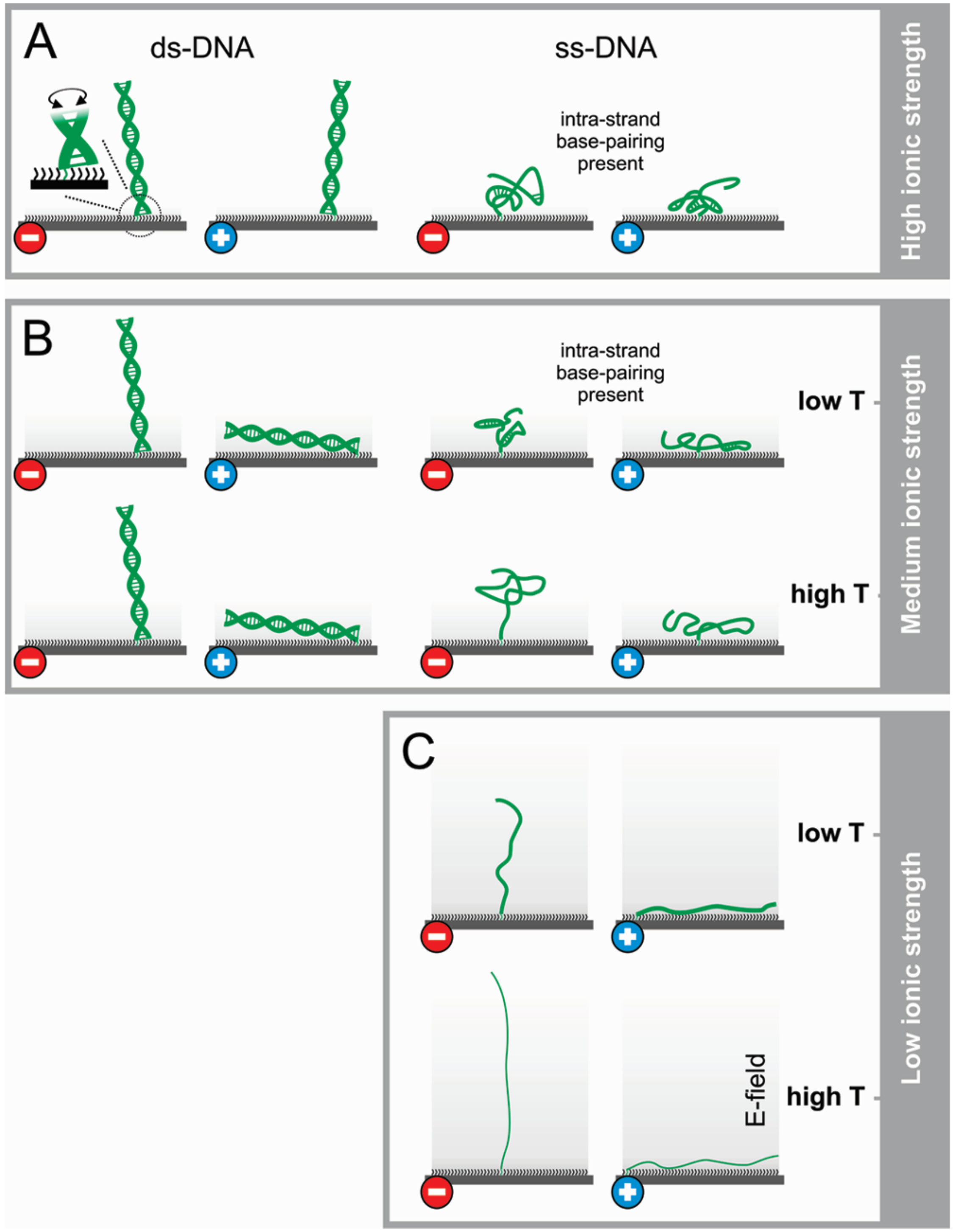

Figure 6. Schematic representation of the DNA conformation on negatively and positively charged surfaces in electrolyte of varying ionic strength.

Kaiser, W.; Rant, U. Conformations of End-Tethered DNA Molecules on Gold Surfaces: Influences of Applied Electric Potential, Electrolyte Screening, and Temperature. J. Am. Chem. Soc 2010, 132 (23), 7935–7945.

References

Some of the references used and others describing the models used in electrochemical double layers. This list is by no means complete.

- Mohilner, D. The Electrical Double Layer. In Electroanalytical Chemistry. A series of advances; Bard, A., Ed.; Marcel-Decker, New York; Vol. 1, pp 241–409.
- Parsons, R. The Structure of the Electrical Double Layer and Its Influence on the Rates of Electrode Reactions. In Advances in Electrochemistry and Electrochemical Engineering; Delahay, P., Tobias, C. W., Eds.; Advances in Electrochemistry and Electrochemical Engineering; interscience: New York, 1966; Vol. 1, pp 1–65.
- Mohilner, D. M.; Beck, T. R. Thermodynamic Theory of Electrocapillarity for Solid Metal Electrodes. The Journal of Physical Chemistry 1979, 83 (9), 1160–1166.
- Parsons, R. Thermodynamic Methods for the Study of Interfacial Regions in Electrochemical Systems. In Comprehensive Treatise of Electrochemistry; Bockris, J. O., Conway, B. E., Yeager, E., Eds.; Comprehensive Treatise of Electrochemistry; Plenum Press: New York, 1980; Vol. 1, pp 1–44.
- Plambeck, J. A. Electroanalytical Chemistry; John Wiley & Sons, 1982.
- Parsons, R. Electrical Double Layer: Recent Experiments and Developments. Chem. Rev. 1990, 90, 813–826.
- Lipkowski, J.; Stolberg, L. Adsorption of Molecules at Metal Electrodes; Lipkowski, J., Ross, P. N., Eds.; Frontiers of Electrochemistry; VCH Publishers Inc., 1992; pp 171–238.
  Bard, A. J.; Abruna, H. D.; Chidsey, C. E. The Electrode/Electrolyte Interface-a Status Report. The Journal of Physical Chemistry 1993, 97 (28), 7147–7173.
- Shi, Z.; Lipkowski, J. Chloride Adsorption at the Au(111) Electrode Surface. J. Electroanal. Chem. 1996, 403 (1-2), 225.
- Guidelli, R.; Schmickler, W. Electrosorption Valency and Partial Charge Transfer. In Modern Aspects of Electrochemistry; Springer, 2013; Vol. 38, pp 303–385.
- Schmickler, W. Interfacial Electrochemistry; Oxford University Press, 1996.
- Schmickler, W. Electronic Effects in the Electric Double Layer. Chem. Rev. 1996, 96 (8), 3177–3200.
- Ataka, K.-I.; Yotsuyanagi, T.; Osawa, M. Potential-Dependent Reorientation of Water Molecules at an Electrode/Electrolyte Interface Studied by Surface-Enhanced Infrared Absorption Spectroscopy. J. Phys. Chem. 1996, 100 (25), 10664–10672.
- Chen, A.; Shi, Z.; Bizzotto, D.; Lipkowski, J.; Pettinger, B.; Bilger, C. Iodide Adsorption at the Au(111) Electrode Surface. J. Electroanal. Chem. 1999, 467 (1-2), 342–353.
- Lipkowski, J.; Szymanski, G.; Chen, A.; Burgess, I.; Bizzotto, D.; Cai, X.; Hoon-Khosla, M.; Jeffrey, C. Spectroscopic and Electrochemical Studies of Coordination of Organic Molecules to Gold Single Crystal Surfaces. NATO Science Series, Series C: Mathematical and Physical Sciences 2000, 546 (Metal-Ligand Interactions in Chemistry, Physics and Biology), 155–181.
- Guidelli, R.; Schmickler, W. Recent Developments in Models for the Interface Between a Metal and an Aqueous Solution. Electrochim. Acta 2000, 45 (15-16), 2317–2338.
- Damaskin, B. B.; Petrii, O. A. Historical Development of Theories of the Electrochemical Double Layer. Journal of Solid State Electrochemistry 2011, 15 (7-8), 1317–1334
- Uchida, T.; Osawa, M.; Lipkowski, J. SEIRAS Studies of Water Structure at the Gold Electrode Surface in the Presence of Supported Lipid Bilayer. J. Electroanal. Chem. 2014, 716, 112–119.